

# **Lab Report 4: Fractals**

By **Sean Alexander**, lab conducted with Cathal Maguire

February 2024

# Contents

<b>1 Abstract</b>	<b>3</b>
<b>2 Theory and Introduction</b>	<b>3</b>
2.1 Introduction to Fractals . . . . .	3
2.1.1 Dense Radial Fractals . . . . .	4
2.1.2 Diffusion-Limited Aggregation Fractals . . . . .	5
2.1.3 Dendritic Fractals . . . . .	6
2.1.4 Stringy Fractals . . . . .	6
2.2 Fractal Dimension . . . . .	6
2.3 Experimental Theory . . . . .	7
2.3.1 Mass Comparison . . . . .	7
2.3.2 Box Counting . . . . .	7
2.3.3 Chemistry Background . . . . .	8
<b>3 Apparatus</b>	<b>8</b>
<b>4 Methodology</b>	<b>9</b>
4.1 Part 1: . . . . .	9
4.2 Part 2: . . . . .	10
<b>5 Data</b>	<b>11</b>
<b>6 Results</b>	<b>13</b>
6.1 Fractal Dimension by method of Mass Comparison . . . . .	13
6.2 Fractal Dimension by method of Box Counting . . . . .	15
<b>7 Error Analysis and Propagation:</b>	<b>18</b>
<b>8 Conclusions</b>	<b>19</b>
<b>9 References / Bibliography:</b>	<b>20</b>
<b>10 Image Appendix:</b>	<b>21</b>

# 1 Abstract

Fractals are abstract mathematical objects, first formulated to describe objects which are not infinitely smooth. The experiment outlined explores the growth patterns and fractal dimensions of zinc deposits formed under varying levels of concentration and voltage. Experimental data was collected using zinc sulfate monohydrate solutions of different molarities subjected to different voltages. Fractal analysis was conducted using two methods: mass comparison and box counting. The results reveal intriguing patterns of fractal growth, with structures ranging from stringy to dense radial formations. Moreover, the fractal dimensions obtained shed light on the complex dynamics underlying the deposition process. Fractal dimensions of fractals grown ranged from  $1.4 \pm 0.1$  to  $1.92 \pm 0.02$ , indicating multifaceted growth patterns influenced by the concentration and voltage parameters.

# 2 Theory and Introduction

## 2.1 Introduction to Fractals

Fractals are abstract mathematical objects originally formulated to describe the roughness of a feature such as the coastline of Britain. The ideal fractal is a mathematical object which contains detailed structure at arbitrarily small scales. It may look the same independent of scale or exhibit the property of self similarity as one views it at increasing or decreasing magnifications. However, like many ideal concepts, the ideal fractal does not have an exact equivalent physical manifestation. Real fractals may exhibit self similarity but in contrast, they always have an upper and lower bound (being the macro-scale deposit size and the assumption of the lower bound existing at or above the atomic scale) and unlike many ideal fractals, they only display statistical self similarity. Despite the inability to physically grow ideal fractals in a lab, one may grow fractals which are not ideal which display structures, many of which have been sorted into the following broad categories: dense radial, diffusion-limited aggregation (DLA), dendritic, and stringy.

### 2.1.1 Dense Radial Fractals

Dense radial fractals grow radially, and appear as shown below:

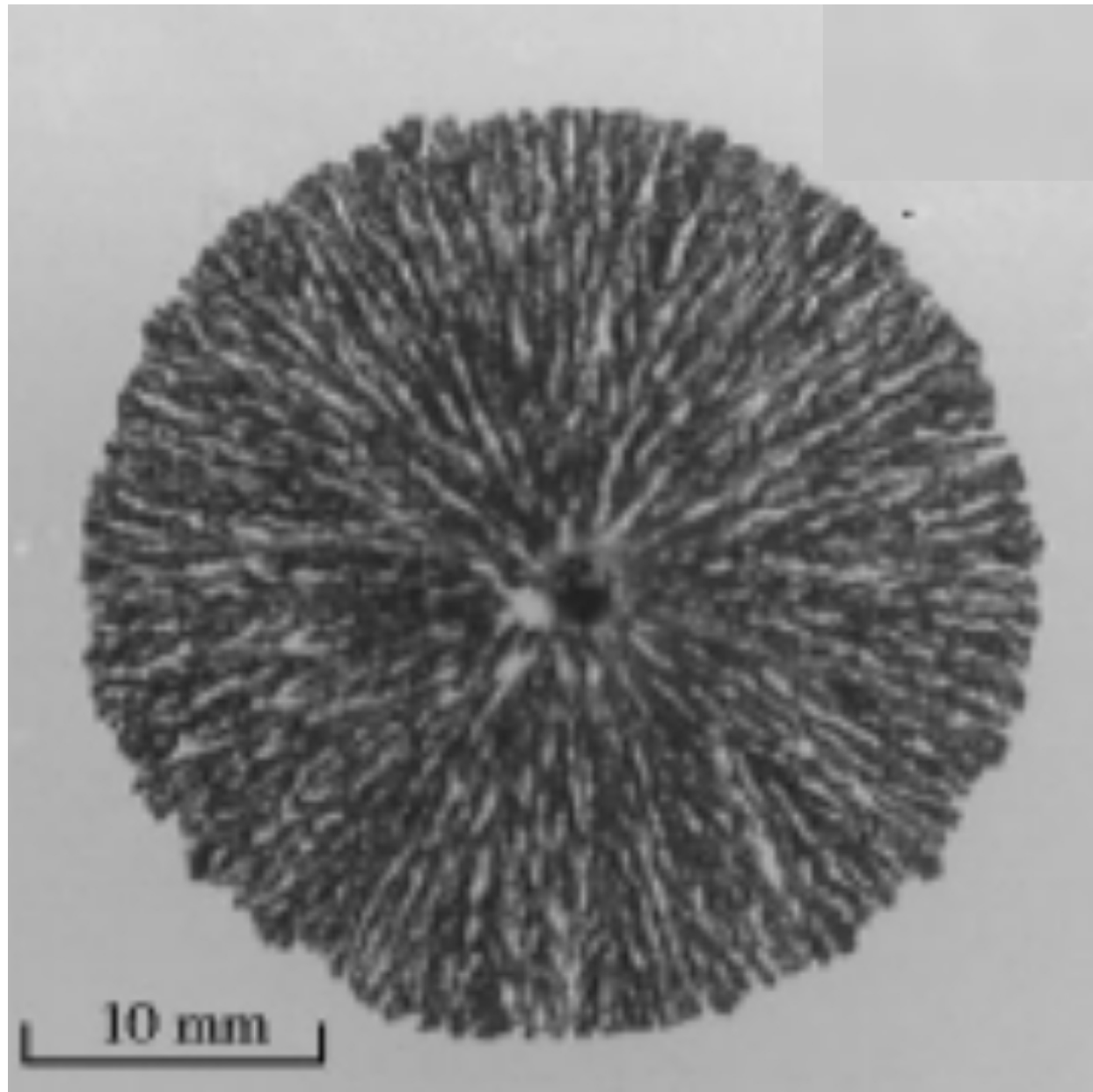


Figure 1: *Dense Radial Fractal Example*

### 2.1.2 Diffusion-Limited Aggregation Fractals

Diffusion-Limited Aggregation fractals grow under low voltage low concentration conditions and appear as shown:

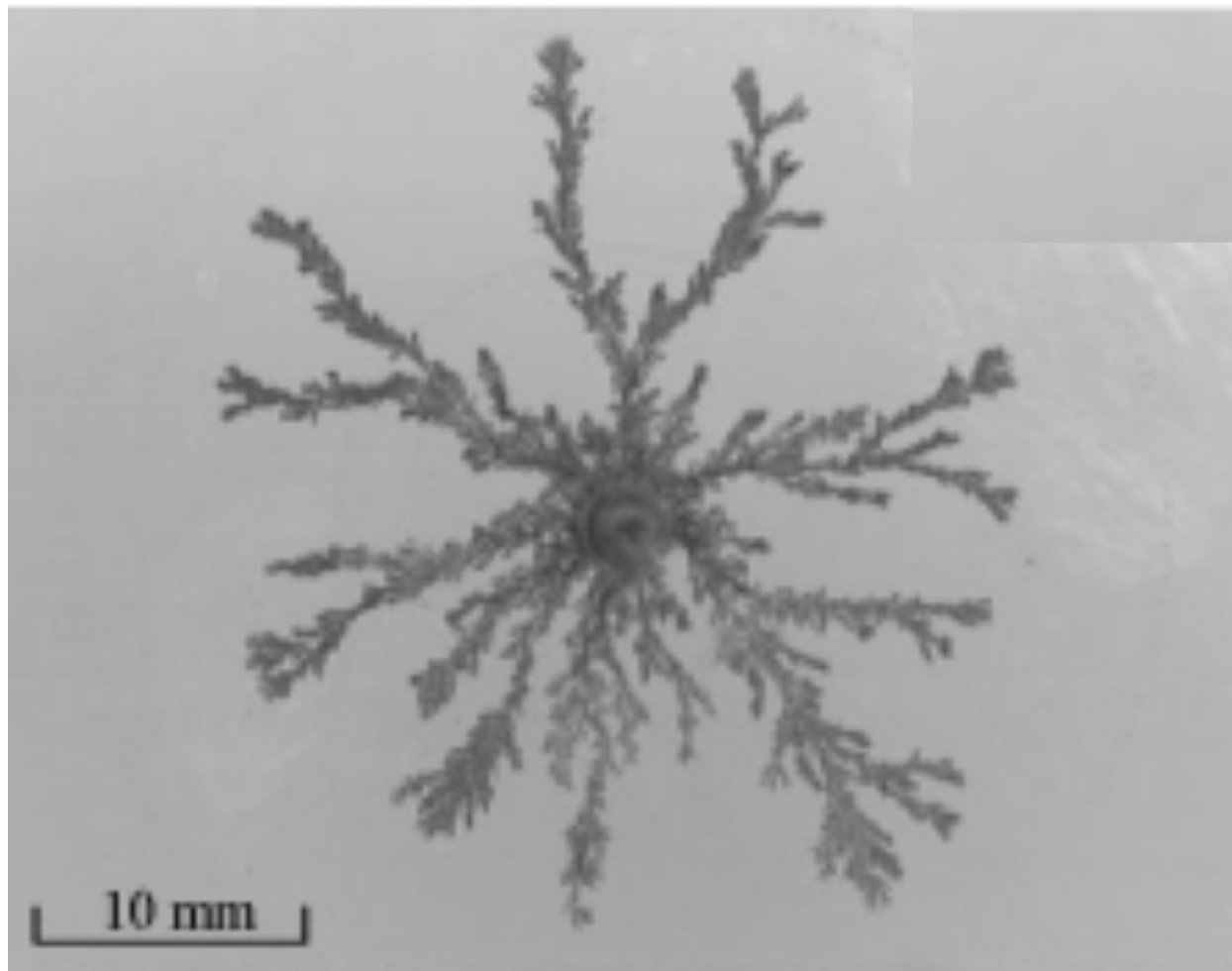


Figure 2: *Diffusion-Limited Aggregation Fractal Example*

### 2.1.3 Dendritic Fractals

Dendritic fractals grow out in a branching structure which ranges from sparse to dense in the amount in branches:

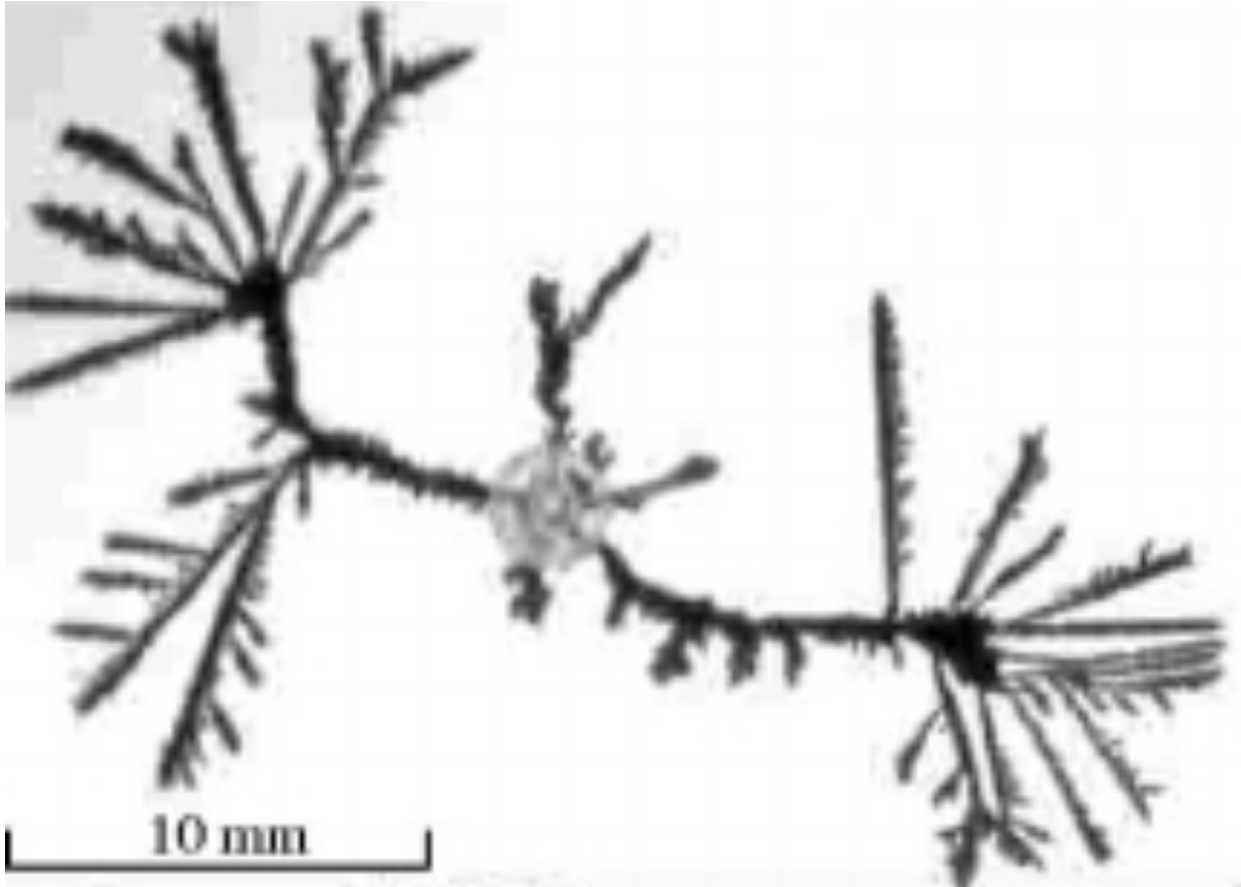


Figure 3: *Dendritic Fractal Example*

### 2.1.4 Stringy Fractals

Stringy fractals grow out primarily in only one or two directions and are the sparse extreme of dendritic fractals. Two examples are present in data Set I achieved during this experiment.

## 2.2 Fractal Dimension

The fractal dimension of an object is easier to understand if one first declares the fractal dimension of some rudimentary geometries. The fractal dimension of a line is equal to 1, while the fractal dimension of a plane is equal to 2. One could describe a fractal dimension  $\mathbb{R}$  as the amount an object fills a space  $\mathbf{R}^{\lceil \cdot \rceil}$  where  $\lceil \cdot \rceil$  denotes the ceiling function. A coastline viewed from above, such as that of Britain is rough enough to act as if it partially fills a planar space which would not be the case if it were entirely straight. The coastline of Britain as viewed from above has a fractal dimension of roughly 1.21 which means the object is rough enough to partially act as if it is a surface rather than a one dimensional line. There are many ways to measure the fractal dimension of an object; two of which explored during the following experiment include mass comparison, and the box counting method. These methods will be described in the **Experimental Theory** section.

## 2.3 Experimental Theory

### 2.3.1 Mass Comparison

The "mass" measured in mass comparison is not mass in the traditional physical sense. The "mass" involved in mass comparison does not require a weighing scale but instead ascribes a homogeneously distributed "mass" to a measured line or area elements and assumes that the "mass" scales proportionally to increases or decreases in measure. This "mass" is then measured at different scales which should increase or decrease in line with the following equation:

$$s^D \cdot M = M' \quad (2.1)$$

Where  $s$  is the scaling factor applied to an object with "mass"  $M$ ,  $D$  is the fractal dimension of the object, and  $M'$  is the mass of the scaled object. Thus the fraction dimension  $D$  is found according to the following equation:

$$D = \frac{\log[\frac{M'}{M}]}{\log[s]} \quad (2.2)$$

Unfortunately, the limits photographic resolution and computational methods forbid us from directly measuring line and area elements of a given physical fractal such that the equation must be adapted. The fractal dimension is instead measured in terms of the number of points ( $N$ ) measured along a radius ( $r$ ) from a given centre. The quotient of the logarithm of the number of points ( $\log[N(r)]$ ) and of the radius ( $\log[r]$ ) is then plotted, and the slope is found using linear regression according to the following equation:

$$D = \frac{\log[N(R)]}{\log[R]} \quad (2.3)$$

### 2.3.2 Box Counting

Another method of determining the fractal dimension is through overlaying a grid of boxes over an image of the fractal and noting the number of boxes that touch the fractal edge at difference scales. This shows how much the scale changes the measured proportional length of the fractal edges. The fractal dimension is then found by plotting the logarithm of the number of boxes touching the fractal edge ( $\ln[N(s)]$ ) against the logarithm of the associated scale ( $\ln[s]$ ), and the slope is found using linear regression according to the following equation:

$$D = \frac{\log[N(s)]}{\log[s]} \quad (2.4)$$

However the method used in the following experiment instead equivalently uses the length of the grid ( $l$ ) in pixels as the input parameter instead as demonstrated in the following equation:

$$D = \frac{\log[N(l)]}{\log[l^{-1}]} \quad (2.5)$$

This achieves the same end.

### 2.3.3 Chemistry Background

The chemical used in the following experiment is zinc sulfate monohydrate ( $\text{ZnSO}_4 \cdot \text{H}_2\text{O}$ ). This is a hydrated form of zinc sulfate ( $\text{ZnSO}_4$ ). The zinc sulfate monohydrate is made part of an aqueous solution in this experiment which means starting with the hydrated form is irrelevant. The zinc from the zinc sulfate is deposited through electrowinning:  $(\text{ZnSO}_4 + 2\text{H}_2\text{O} \rightarrow \text{Zn} + \text{SO}_4^{2-} + \text{O}_2 + 4\text{H}^+)$  such that the zinc is deposited on the cathode from the solution. The graphite used in this experiment is attached to the cathode of the battery and immersed in solution such that the zinc is deposited on it instead of the metallic cathode whilst the battery anode is attached to a iron conducting ring surrounding the solution. In order to determine how the zinc deposition changes under different initial concentrations of zinc sulfate monohydrate, a 1 molar concentration is made. This is then followed by (by method of dilution), the formulation of a 0.5, 0.1, and 0.01 molar concentrated solutions. This is done with deionised water and clean graduated glassware to ensure purity is preserved, and is functionally achieved by finding the molecular mass of the zinc sulfate monohydrate, and putting that same number of grams of the chemical into solution such that there is 1 mole of the substance per litre.

## 3 Apparatus

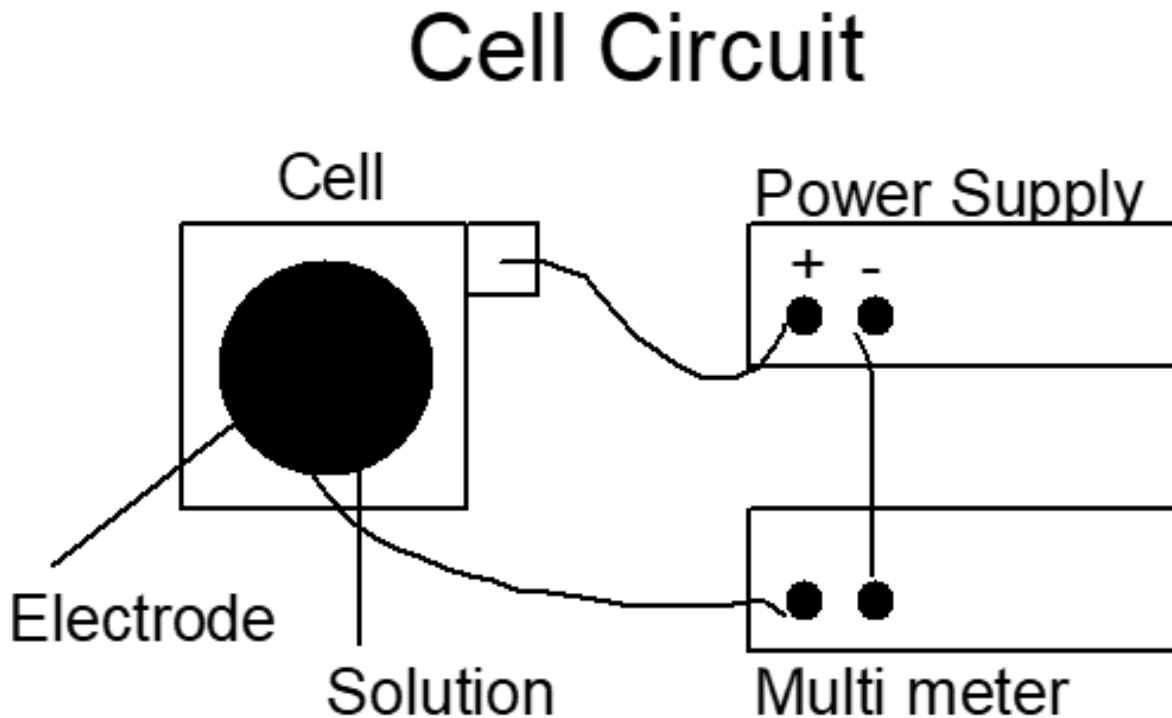


Figure 4: *Circuit Diagram of Apparatus*

- Deionised Water
- Power Supply with varying voltage
- Zinc Sulfate Monohydrate

- Mass Scale
- Perspex Glass (P.G) Cell with P.G Cover with central hole
- Conducting metal ring
- Graphite (0.5 mm Pencil Lead)
- Desktop CCD Camera
- Desktop Computer with Windows Camera App, ImageJ software, and BENOIT<sup>TM</sup> software

## 4 Methodology

In order to achieve the aims outlined in the following sections below::

- The formulation of 1, 0.5, 0.1, & 0.01 molar solutions of Zinc Sulfate was required. This was performed through use of the property of a mole of a substance being that its mass in grams is the same value as its molecular mass.
- The mass scale and deionised water were used to create a solution of one mole per litre concentration and portions of this initial 1 molar solution were diluted to achieve the other desired concentrations.
- These concentrations were then poured into a dip in the perspex glass cells, around which the iron conducting metal plate was added. This was crowned with the P.G cover.
- The cathode of the power supply was connected to the graphite which was threaded through the hole in the P.G cover such that it was in contact with the solution.
- The anode of the power supply was then connected to the conducting metal ring. The power supply was used with measured voltages to grow zinc deposits which grew from the graphite cathode out towards the iron ring anode. These deposits were left grow until they appeared to stop or until they reached a diameter of approximately 3-6 cm.
- The fractals were imaged and their associated voltage and molarities were noted.

### 4.1 Part 1:

The aims of **Part 1** include:

1. To capture images of the grown fractals.
2. To process the fractal images in preparation for BENOIT<sup>TM</sup> software analysis.

In order to achieve the goals outline above:

- The Windows Camera App and the CCD camera were used to capture images of the fractals.
- This camera was positioned such that the crosshairs were at the centre of the fractal above a white background, and the image contrast and resolution could be maximised.
- The images were cropped such that the metal conducting ring were not present in the images while maintaining 4:3 image dimension.

- The images were saved and the ImageJ software was then used to adjust the image brightness and contrast to maximise the contrast between the fractal and the background.]
- The ImageJ software was then used to set the image to greyscale, to invert the images colours such that the BENOIT<sup>TM</sup> software could view the fractal as a white object rather than its natural grey colouring.
- ImageJ software's coordinate tools were then used to note where the centre of the fractal was in terms of X, Y coordinates (This was not always where the graphite cathode was located in the image).
- Finally, the fractal images was saved in the BMP image format.

#### 4.2 Part 2:

The aims of **Part 2** include:

1. Determination of fractal dimension by method of mass comparison using BENOIT<sup>TM</sup> software.
2. Determination of fractal dimension by method of box counting using BENOIT<sup>TM</sup> software.

In order to achieve the goals outline above:

- The mass comparison method was selected, and applied to the fractal images with their noted pixel centres. This was then repeated for some of the images with an offset from the centre to indicate the importance of selecting the correct centre.
- The measured fractal dimension plot was captured and the measured slope and its standard deviation was noted in each case.
- The box counting method was selected, and applied.
- The measured fractal dimension plot was captured and the measured slope and its standard deviation was noted in each case.
- The Fractal Images were classified and plotted on a phase diagram of Voltage and Solute Concentration.
- This data was used in order to morphologically classify the fractals in terms of their starting conditions.

## 5 Data

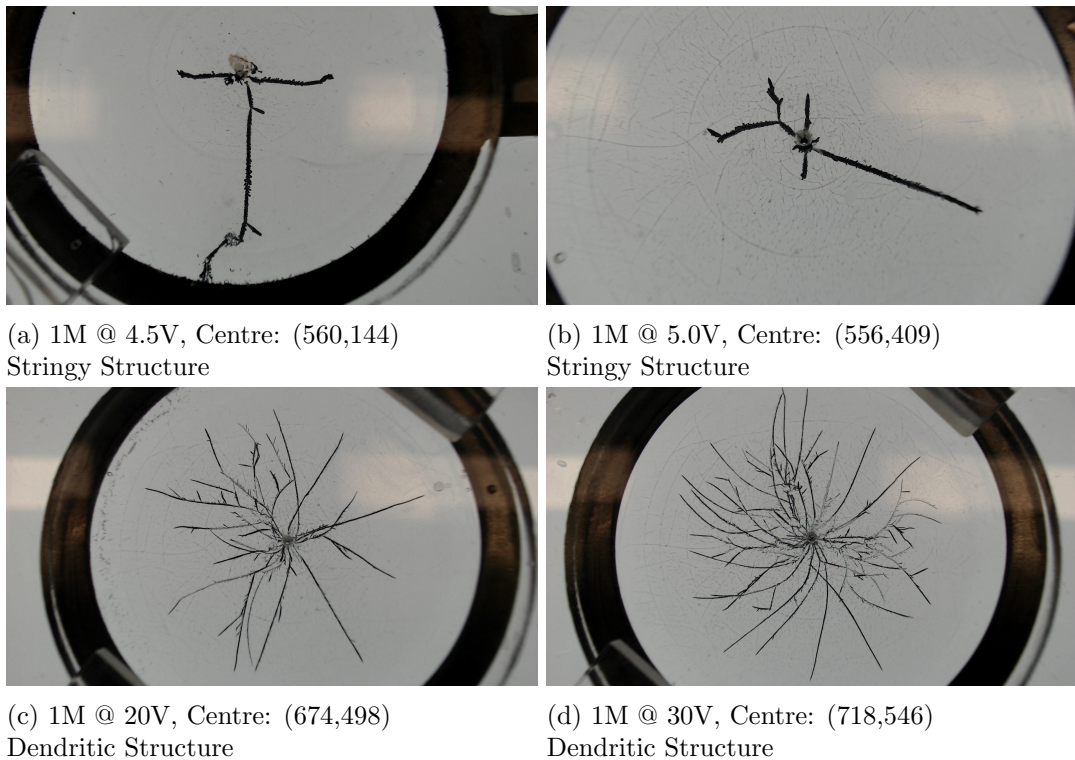


Figure 5: Data Set I.

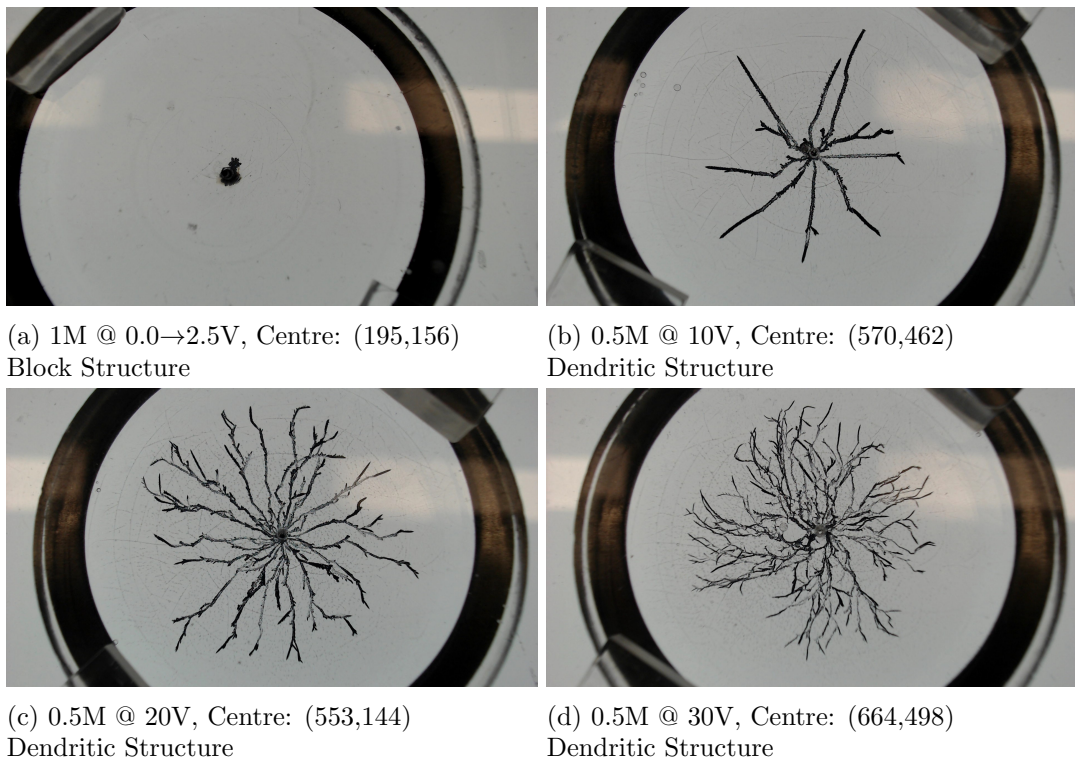


Figure 6: Data Set II.

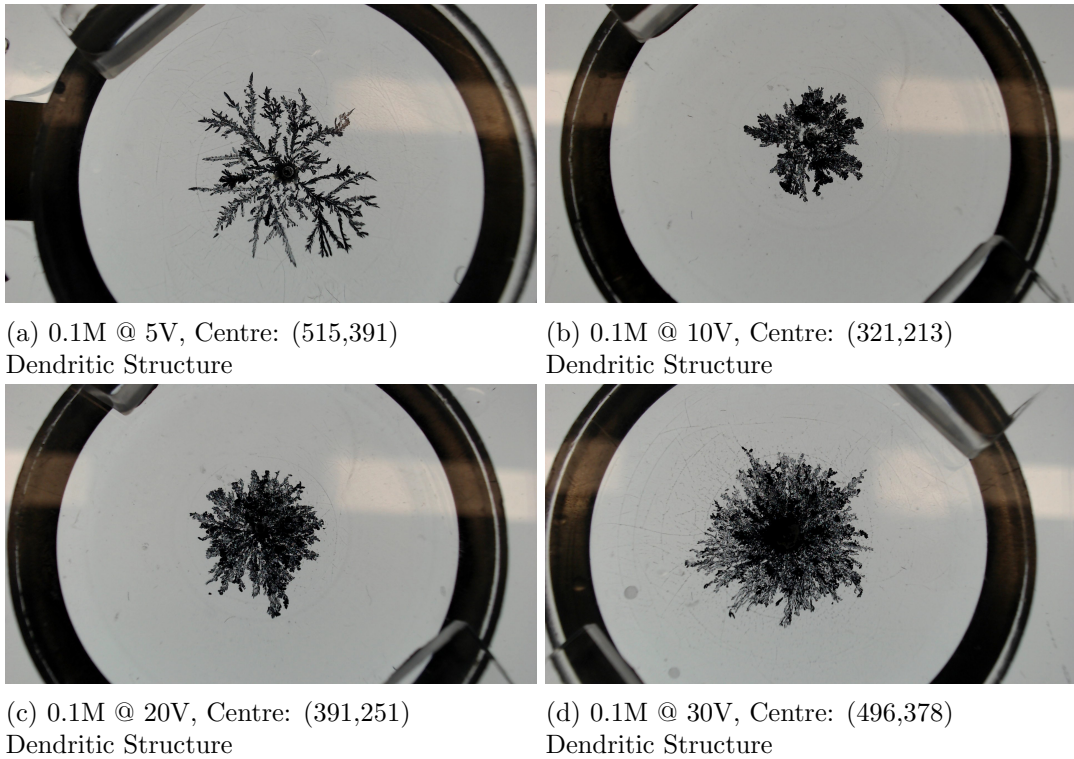


Figure 7: Data Set III.

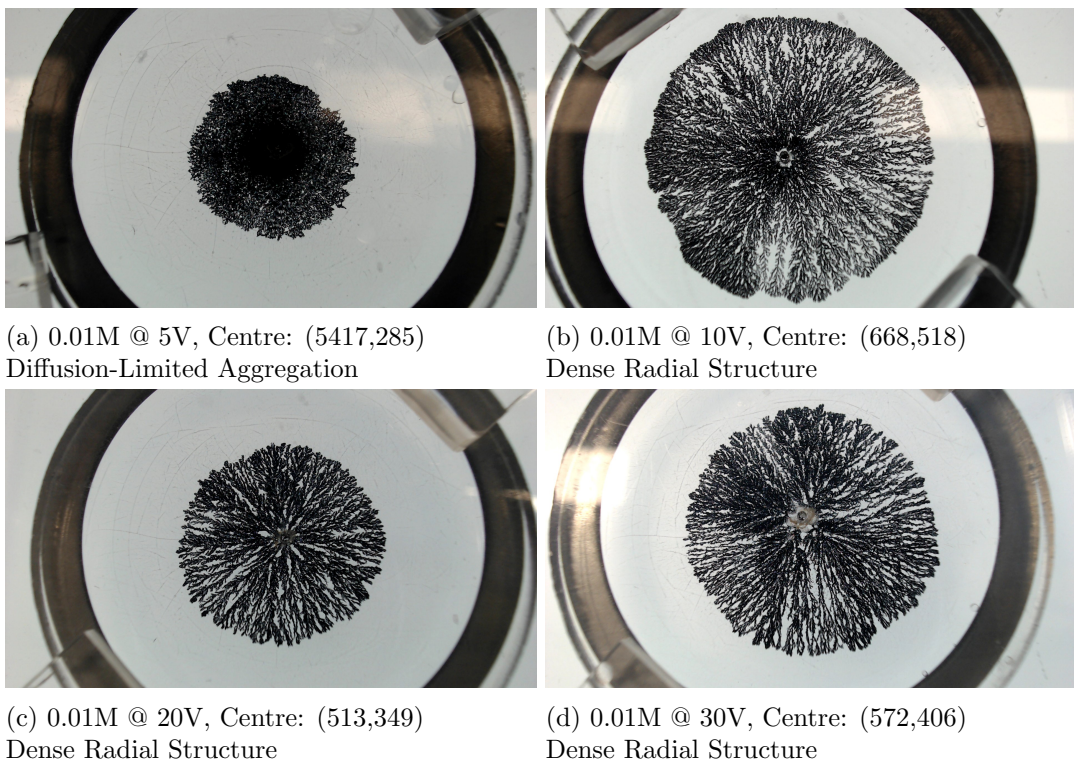


Figure 8: Data Set IV.

## 6 Results

### 6.1 Fractal Dimension by method of Mass Comparison

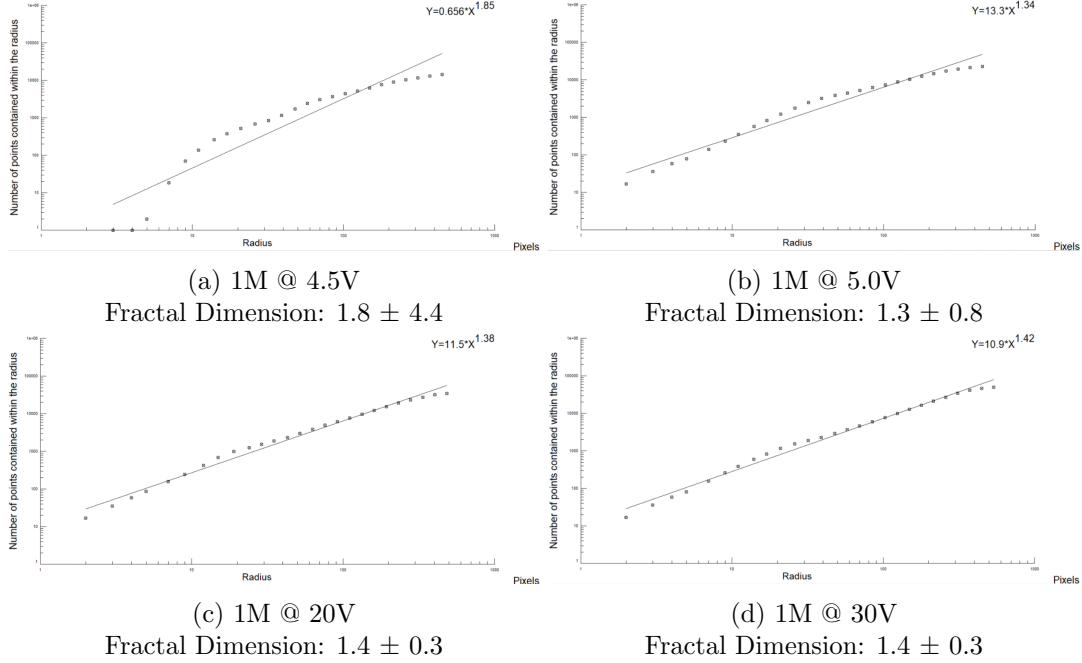


Figure 9: Mass Comparison: Data Set I.

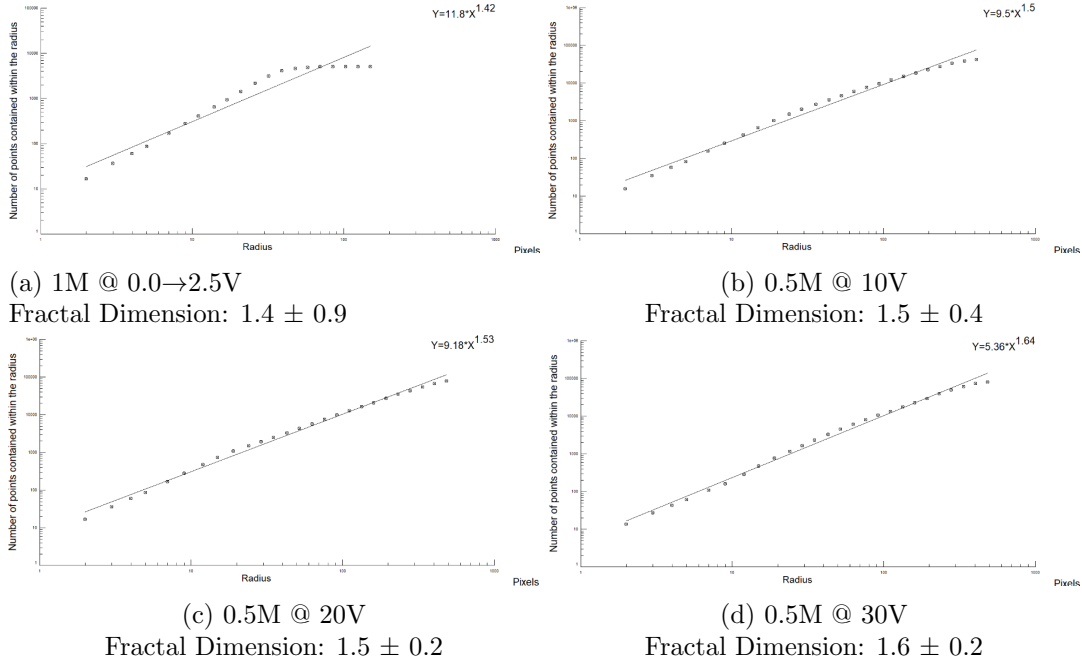


Figure 10: Mass Comparison: Data Set II.

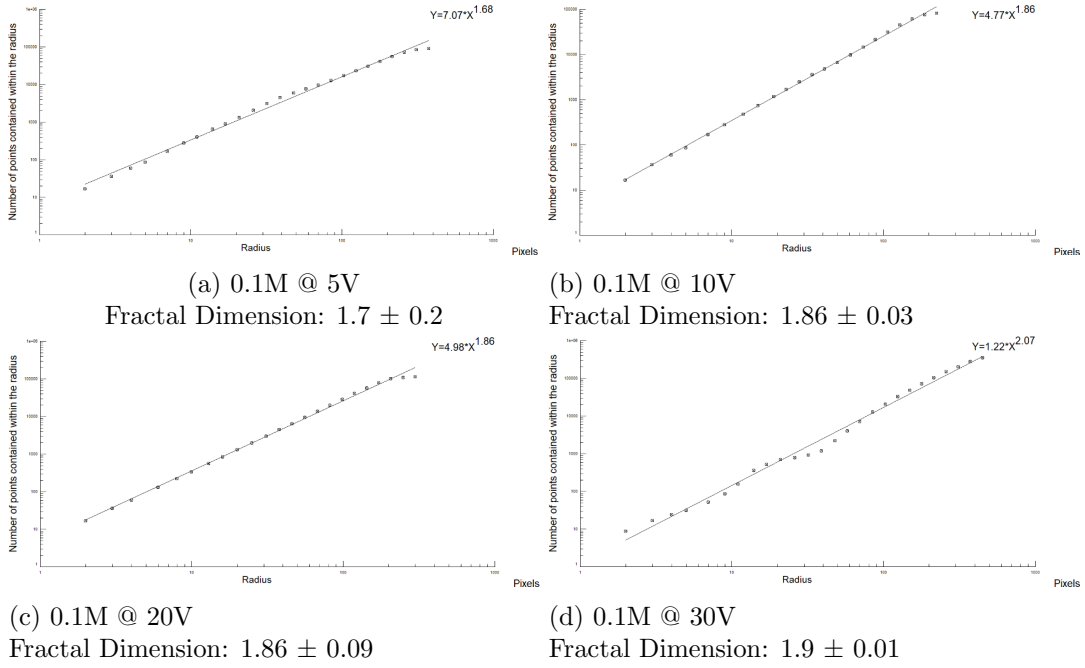


Figure 11: Mass Comparison: Data Set III.

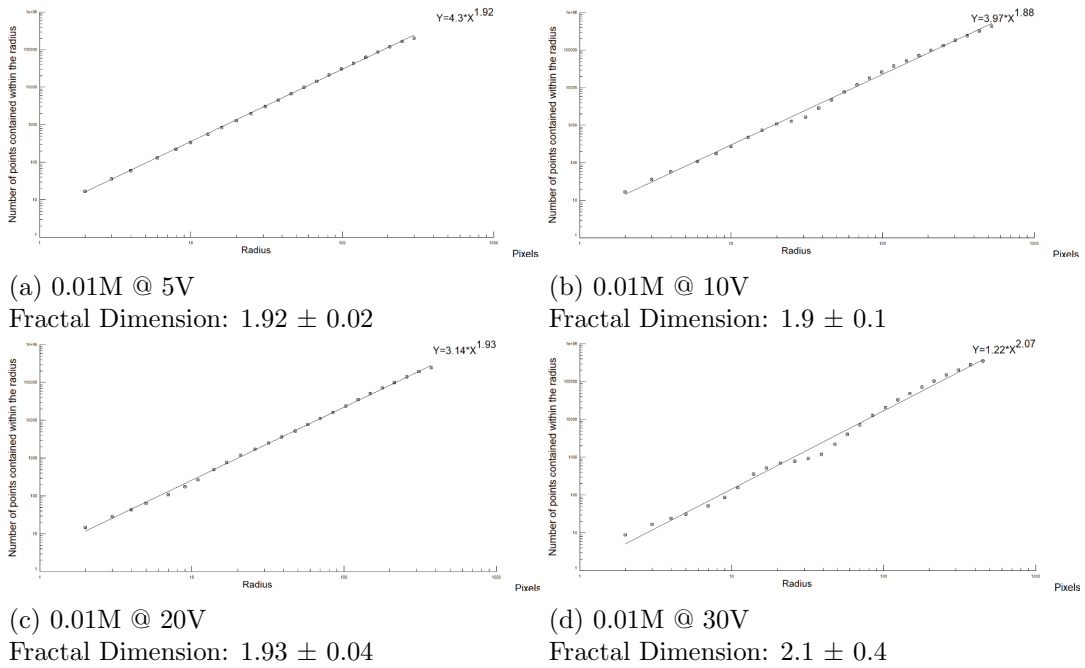


Figure 12: Mass Comparison: Data Set IV.

## 6.2 Fractal Dimension by method of Box Counting

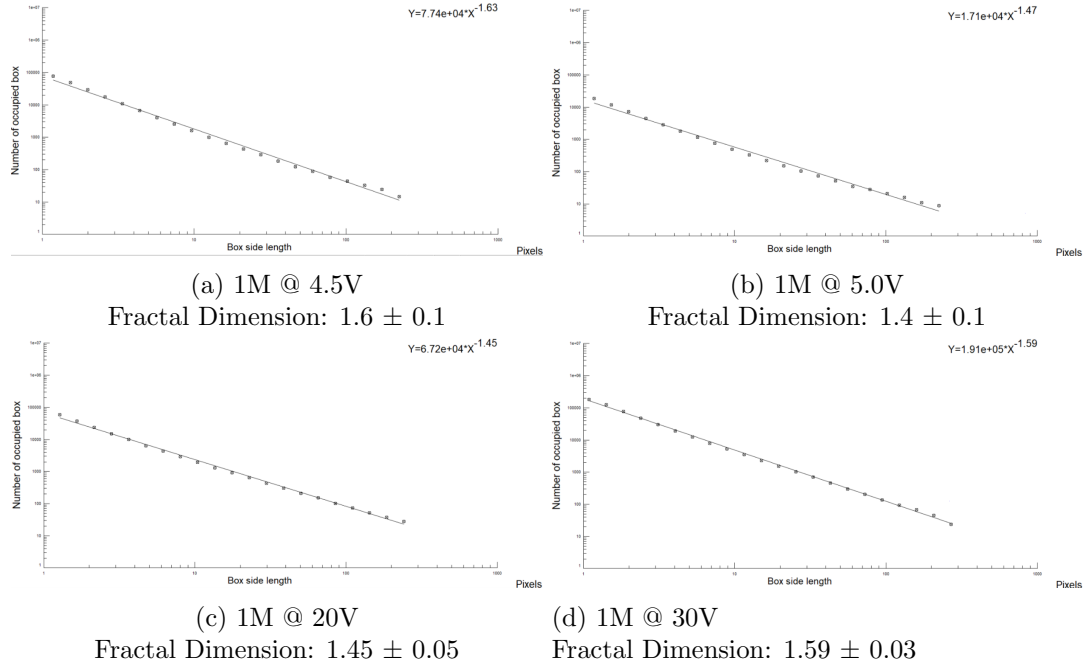


Figure 13: Box Counting: Data Set I.

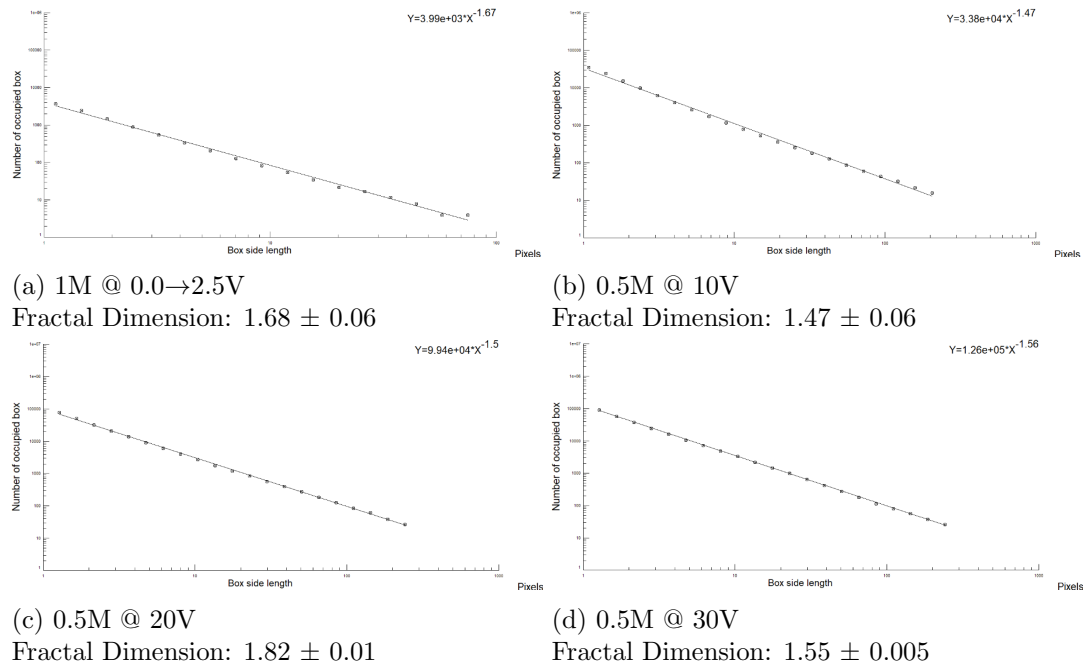


Figure 14: Box Counting: Data Set II.

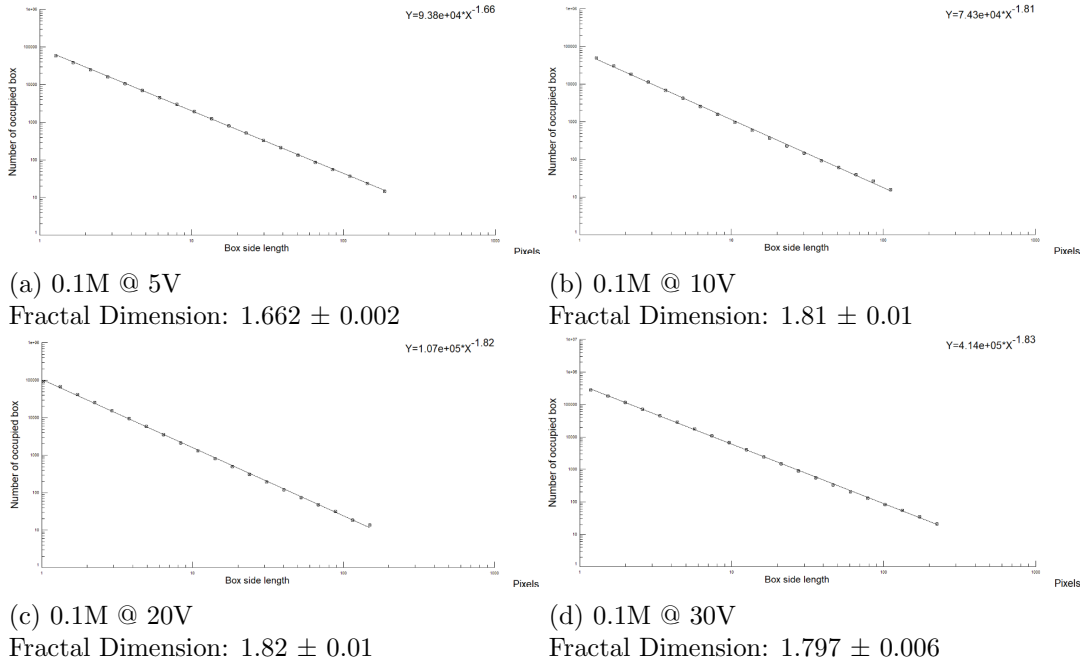


Figure 15: Box Counting: Data Set III.

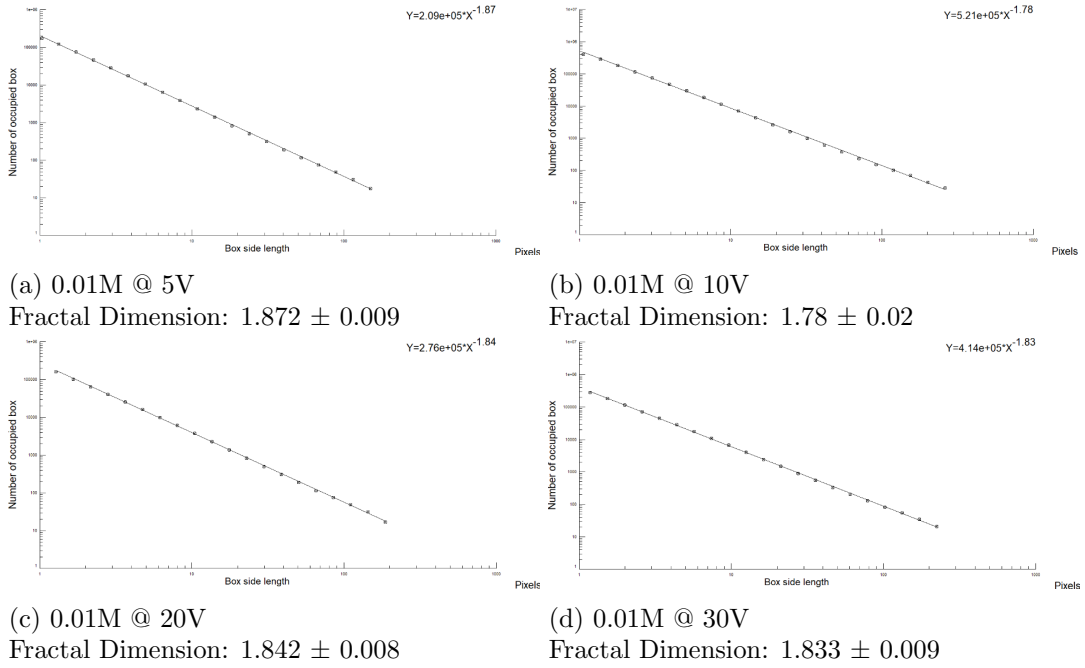


Figure 16: Box Counting: Data Set IV.

The results above indicate that the fractal dimension as calculated by box counting method has a smaller standard deviation and thus it can be extrapolated that it is therefore of lower error and greater efficacy. These results confirm that the low voltage, high molarity regime contains fractals with a stringy structure. The low voltage, low molarity regime produces diffusion-limited aggregations. The rest of the low molarity regime contained dense radially structured fractals while the rest of the population was made of dendritically structured fractals. This is outlined in the phase diagram below.

### Classification of Fractals by Solute Concentration & Applied Voltage

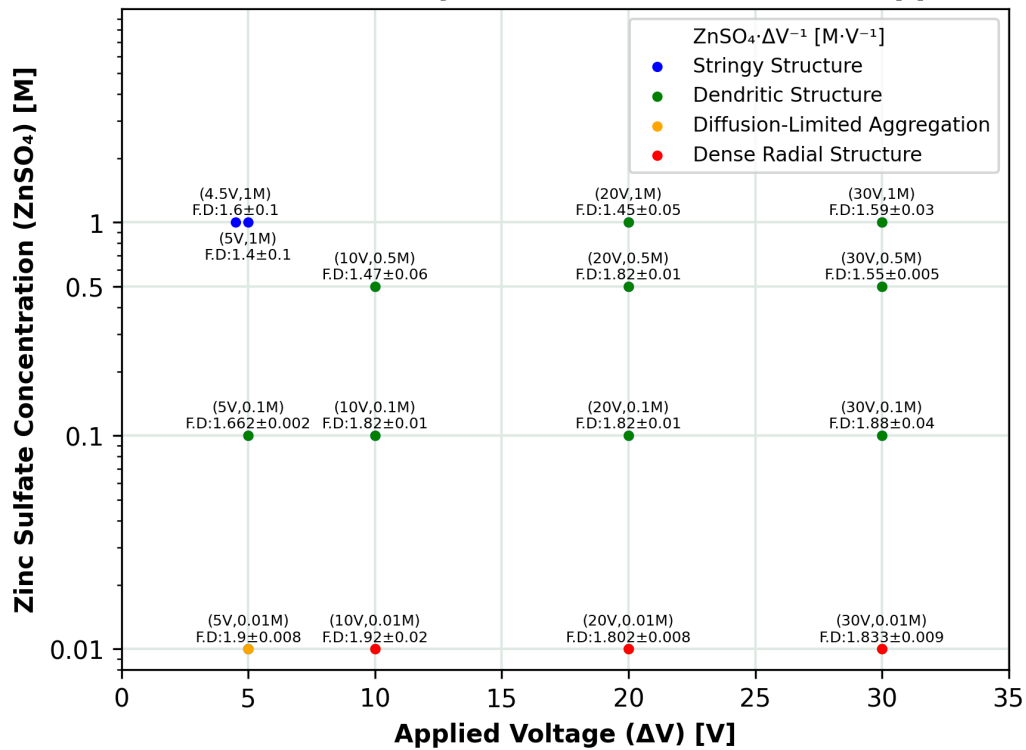


Figure 17: Classification of Fractals by Solute Concentration & Applied Voltage

The fractal dimension of the following image of a snowflake was also found:



Centre: (278,285), F.D by M.C:  $1.83 \pm 0.05$ , F.D by B.C:  $1.775 \pm 0.006$

Figure 18: *Snowflake Fractal from New York Times*

This snowflake image had similar fractal dimension calculated values to dense dendritic structures which aligns well with theory.

## 7 Error Analysis and Propagation:

The standard deviation ( $\sigma$ ) for the fractal dimension as calculated by mass comparison and box counting methods was calculated by the BENOIT™ software and taken as the error of the associated measurements. This may be problematic in some respects as the fractal dimension of a fractal may differ as the scale changes which results in a varying fractal dimension but for the purposes of this experiment, the fractal dimension will be assumed to be constant. A weighted average was then made between the two F.D calculations and it was this weighted average ( $\bar{x}$ ) and error ( $\sigma_{\bar{x}}$ ) which was included in the fractal classification diagram.

These weighted values were calculated as shown below:

$$\bar{x} = \sum_i w'_i \cdot x_i \quad (7.1)$$

Where:

$$w'_i = \frac{\sigma_i^{-2}}{\sum_i \sigma_i^{-2}} \quad (7.2)$$

$x_i$  is the value and  $w'_i$  is the normalized weight associated with value  $x_i$ . The error associated with this method ( $\sigma_{\bar{x}}$ ) was calculated as shown below:

$$\sigma_{\bar{x}} = \sqrt{\sum_i (w'_i)^2 \times \sigma_i^2} \quad (7.3)$$

In order to determine the dependence of the fractal dimension by mass comparison on the provided centre, the fractal dimension analysis of the following fractals was repeated with a different provided centre:

Fractal Parameters	0.01M, 5V	1M, 4.5V
Original Centre	(417,285)	(560,144)
Original F.D	$1.92 \pm 0.02$	$1.8 \pm 4.4$
New Centre	(422,290)	(565,149)
New F.D	$1.92 \pm 0.01$	$1.3 \pm 0.3$

Table 1: Effect of Moving Centre on Value of Fractal Dimension by method of Mass Comparison.

The effect of changing the centre resulted in better overall measurements in both cases with smaller standard deviations. This is an indicator that some of the centres chosen were in-optimal for the calculations of fractal dimension by mass comparison. If this experiment were to be repeated, greater care and importance must be given to the choice of the fractal centre.

## 8 Conclusions

In conclusion, the measurement of fractal dimension using both mass comparison and box counting methods was achieved with varying degrees of success. Measurements indicated that larger applied voltages and higher solute molarities lead to higher measured fractal dimensions. This suggested more complex fractals are formed at higher voltage / solute concentration. However, the reliability of the measurements varied depending on the method used and the type of fractal formed. The phase diagram of the fractal data showed clear distinctions between the different types of fractals formed at different solute concentrations, suggesting that solute concentration has a significant effect on fractal morphology. Overall, the experiment provided valuable insights into the formation of fractals and the factors that influence their morphology.

## 9 References / Bibliography:

[https://www.researchgate.net/publication/8463823\\_Chirality\\_of\\_electrodeposits\\_grown\\_in\\_a\\_magnetic\\_field](https://www.researchgate.net/publication/8463823_Chirality_of_electrodeposits_grown_in_a_magnetic_field) [Accessed February 26th]

Mandelbrot, B.B. (1982) The Fractal Geometry of Nature. Freeman Press, New York

## List of Figures

1	<i>Dense Radial Fractal Example</i> . . . . .	4
2	<i>Diffusion-Limited Aggregation Fractal Example</i> . . . . .	5
3	<i>Dendritic Fractal Example</i> . . . . .	6
4	<i>Circuit Diagram of Apparatus</i> . . . . .	8
5	Data Set I. . . . .	11
6	Data Set II. . . . .	11
7	Data Set III. . . . .	12
8	Data Set IV. . . . .	12
9	Mass Comparison: Data Set I. . . . .	13
10	Mass Comparison: Data Set II. . . . .	13
11	Mass Comparison: Data Set III. . . . .	14
12	Mass Comparison: Data Set IV. . . . .	14
13	Box Counting: Data Set I. . . . .	15
14	Box Counting: Data Set II. . . . .	15
15	Box Counting: Data Set III. . . . .	16
16	Box Counting: Data Set IV. . . . .	16
17	<i>Classification of Fractals by Solute Concentration &amp; Applied Voltage</i> . . . . .	17
18	<i>Snowflake Fractal from New York Times</i> . . . . .	18

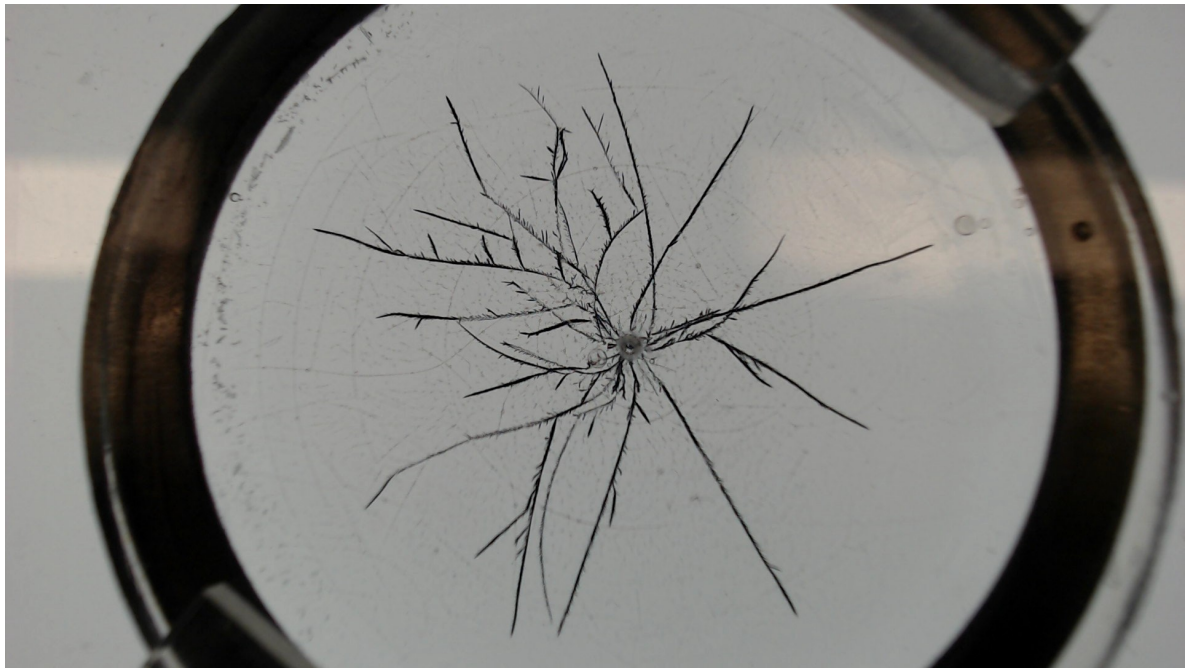
## 10 Image Appendix:



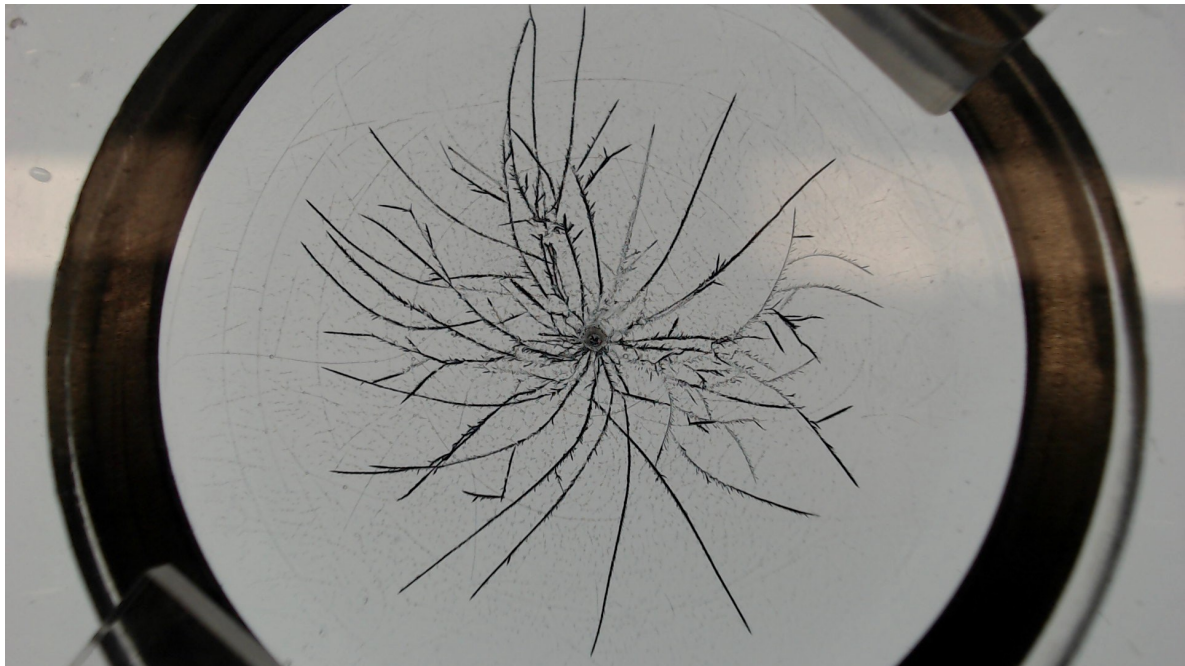
1M @ 4.5V, Centre: (560,144)  
Stringy Structure



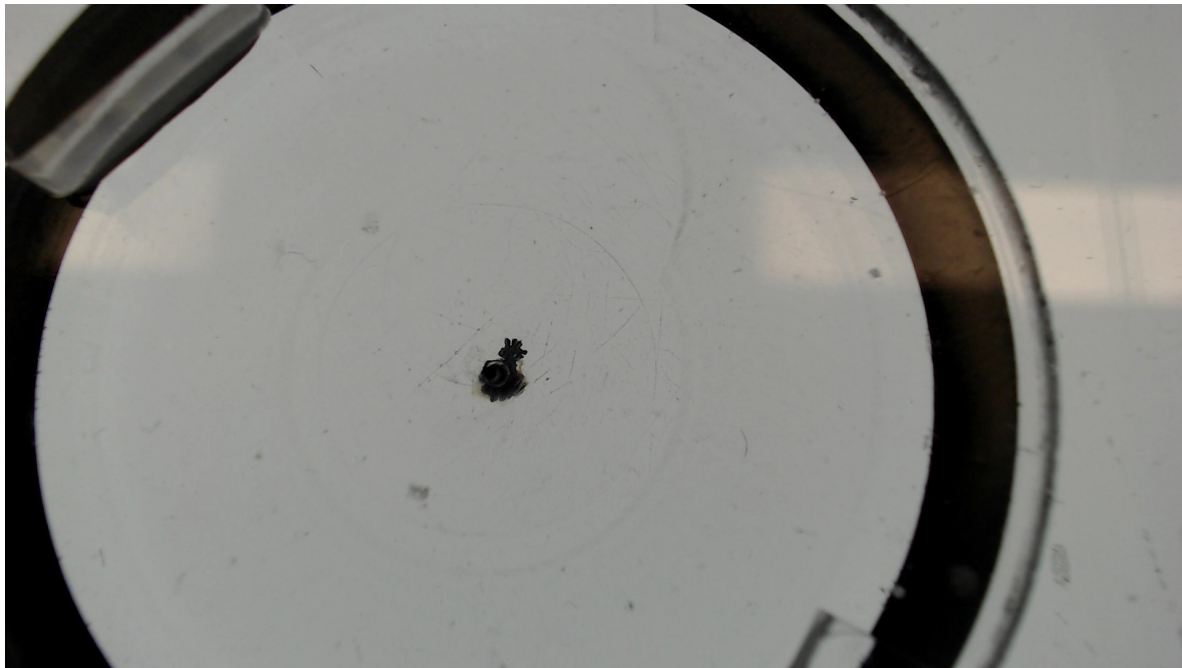
1M @ 5.0V, Centre: (556,409)  
Stringy Structure



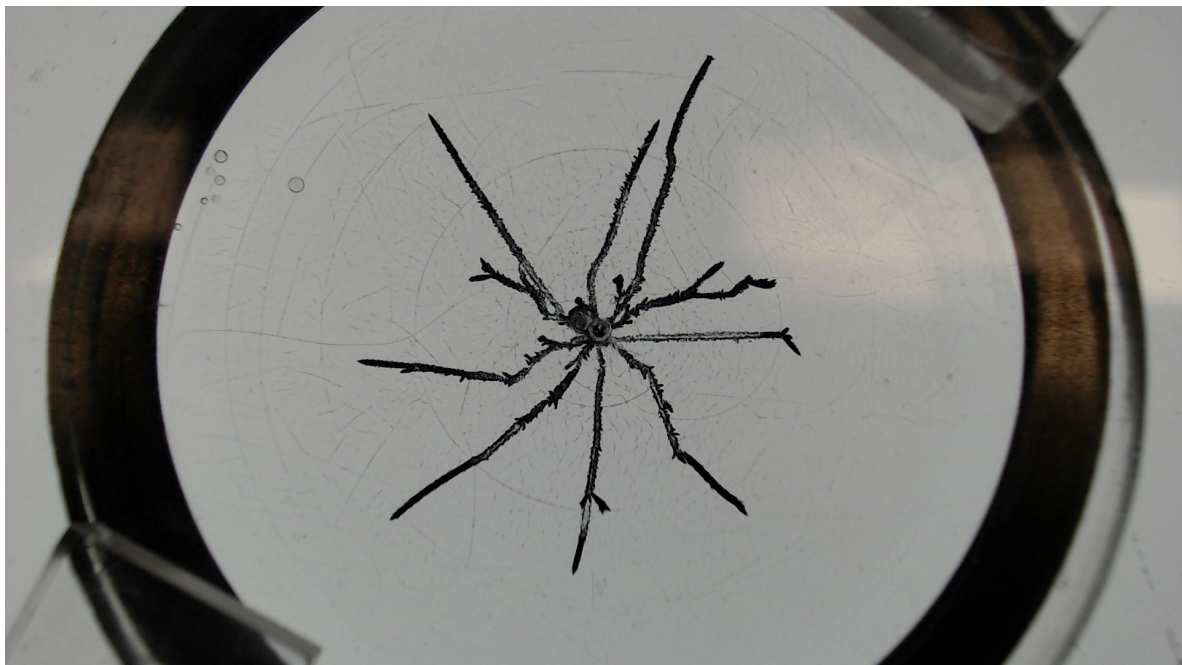
1M @ 20V, Centre: (674,498)  
Dendritic Structure



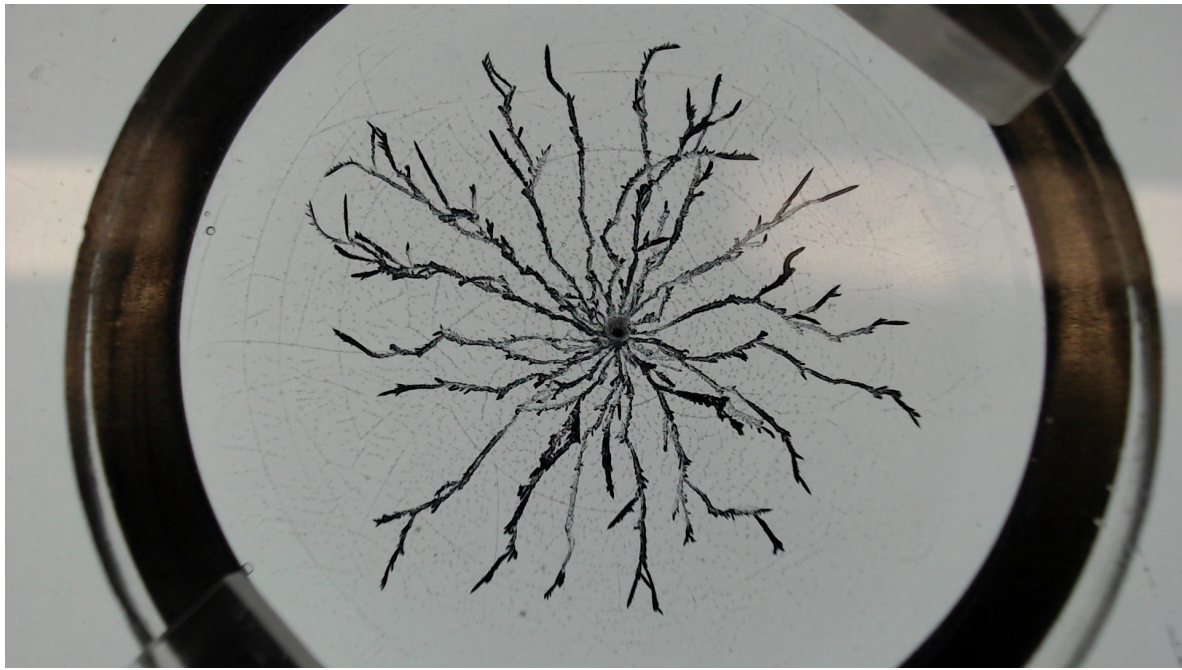
1M @ 30V, Centre: (718,546)  
Dendritic Structure



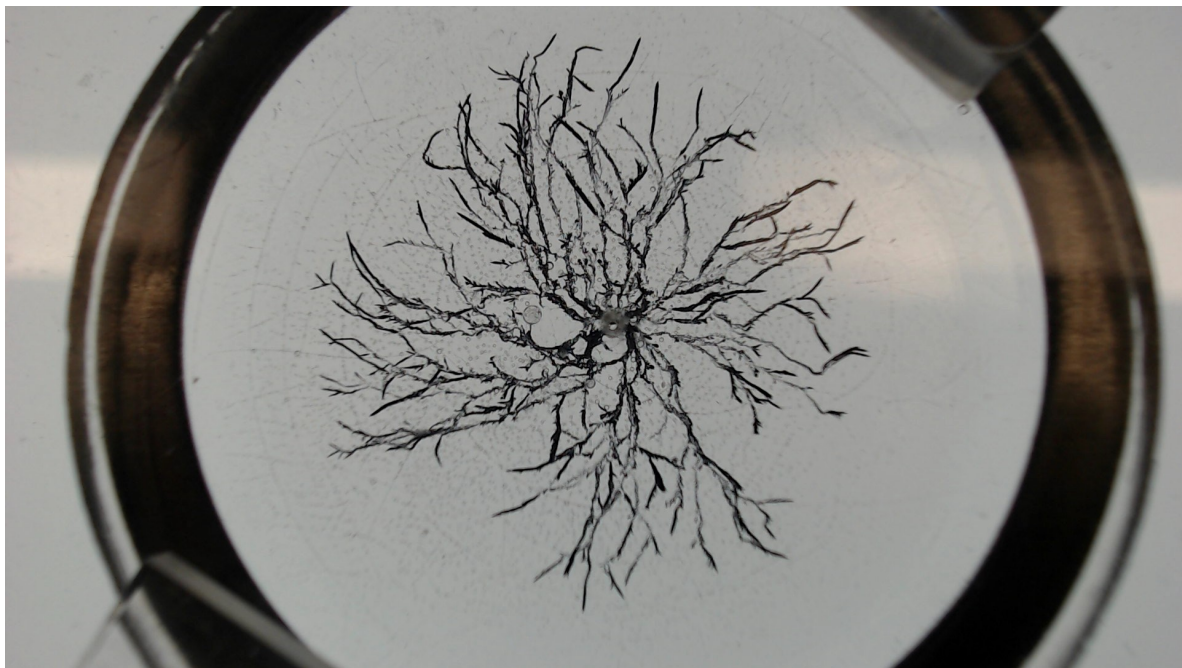
1M @ 0.0→2.5V, Centre: (195,156)  
Block Structure



0.5M @ 10V, Centre: (570,462)  
Dendritic Structure



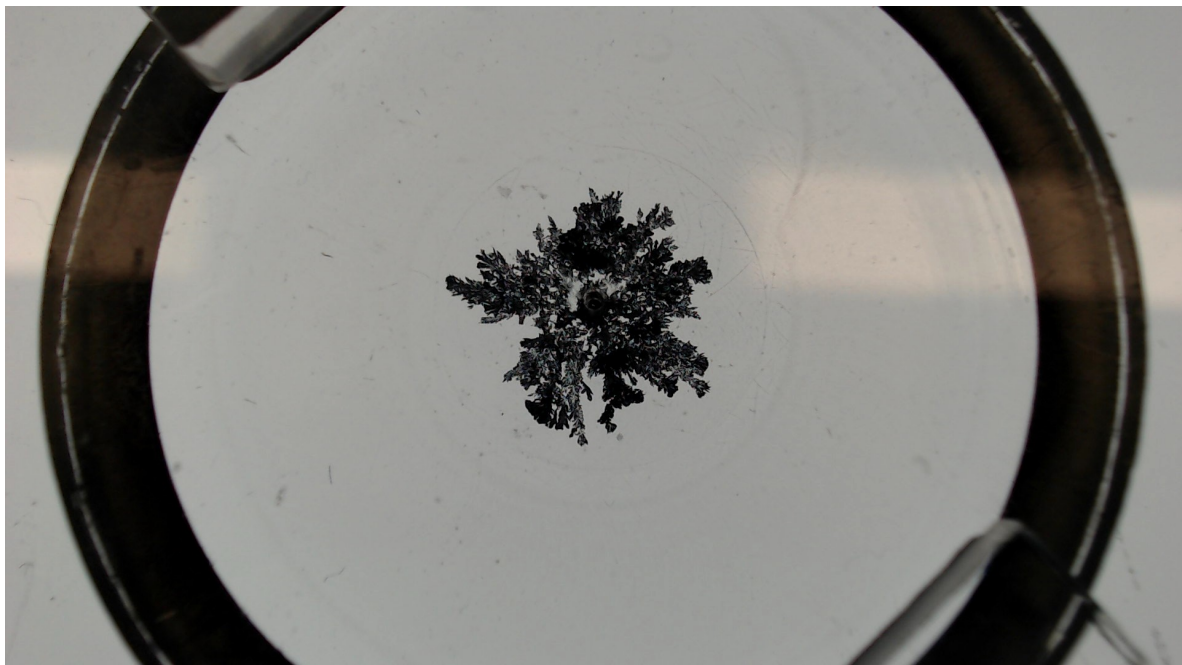
0.5M @ 20V, Centre: (553,144)  
Dendritic Structure



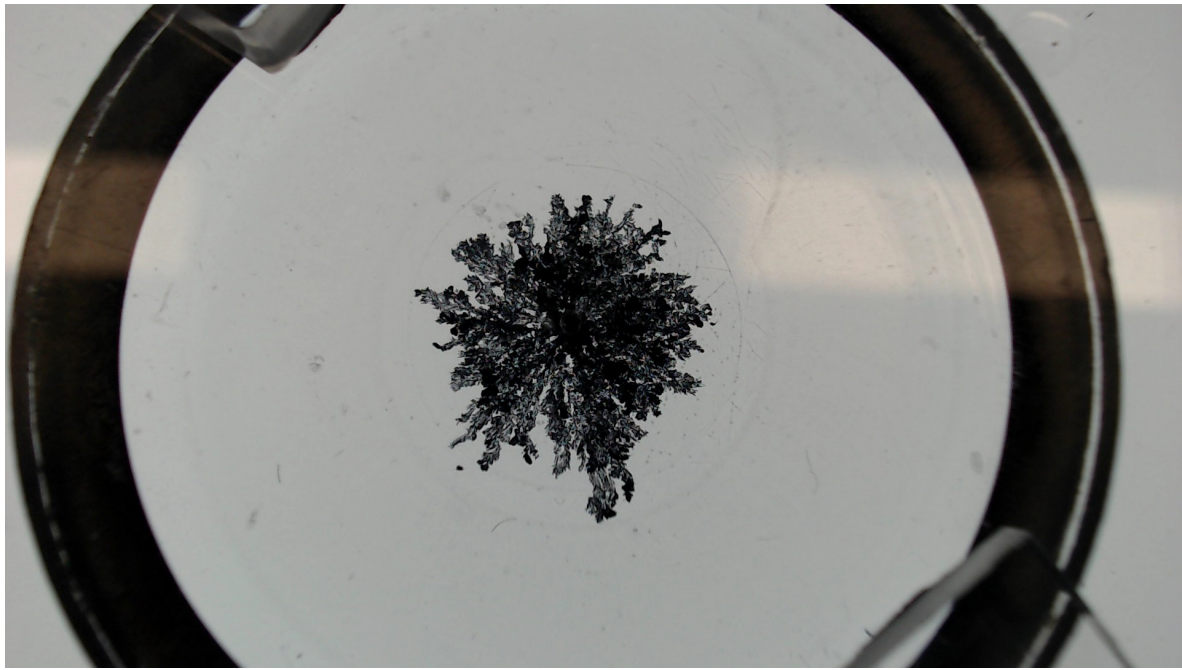
0.5M @ 30V, Centre: (664,498)  
Dendritic Structure



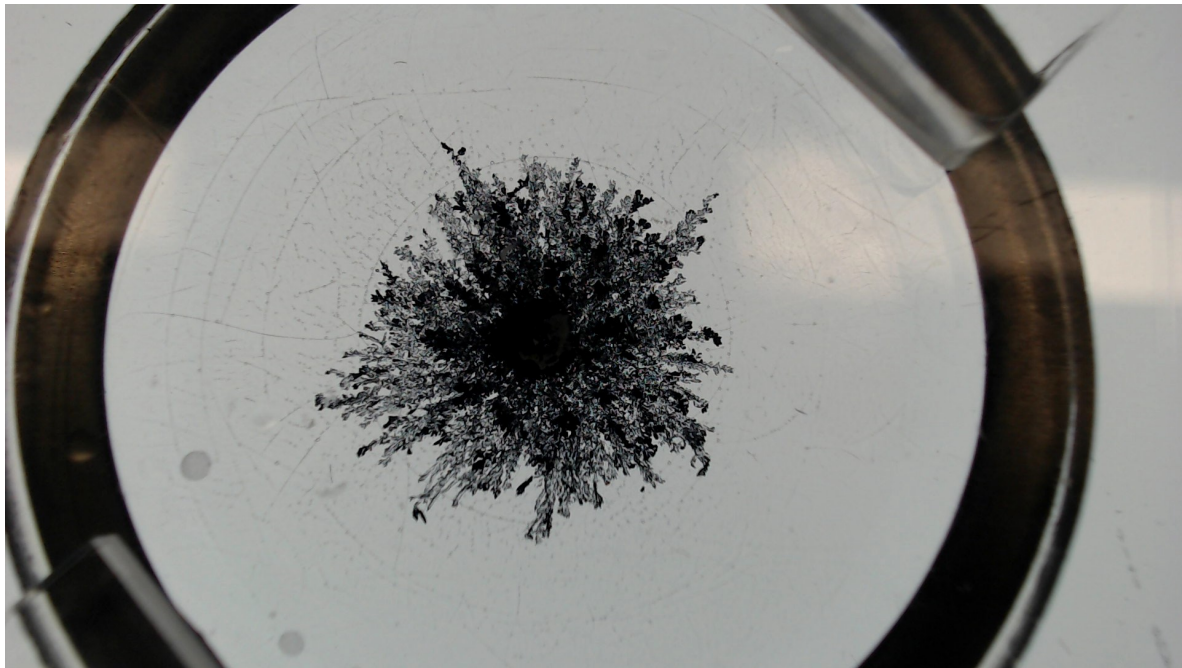
0.1M @ 5V, Centre: (515,391)  
Dendritic Structure



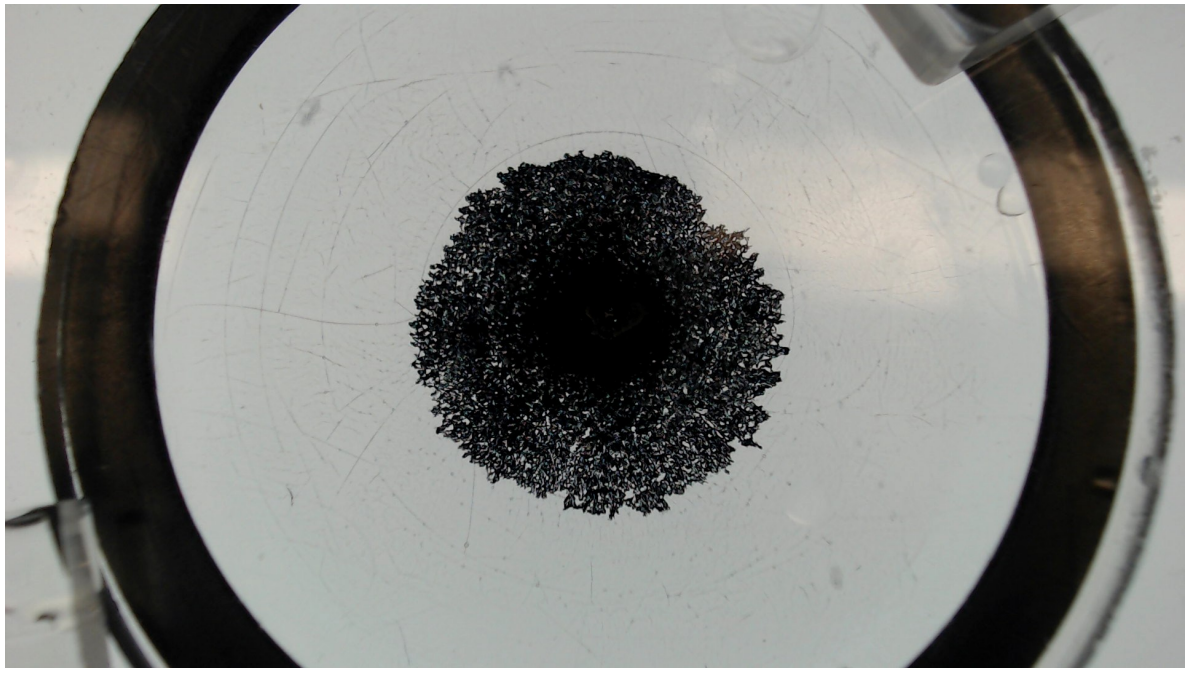
0.1M @ 10V, Centre: (321,213)  
Dendritic Structure



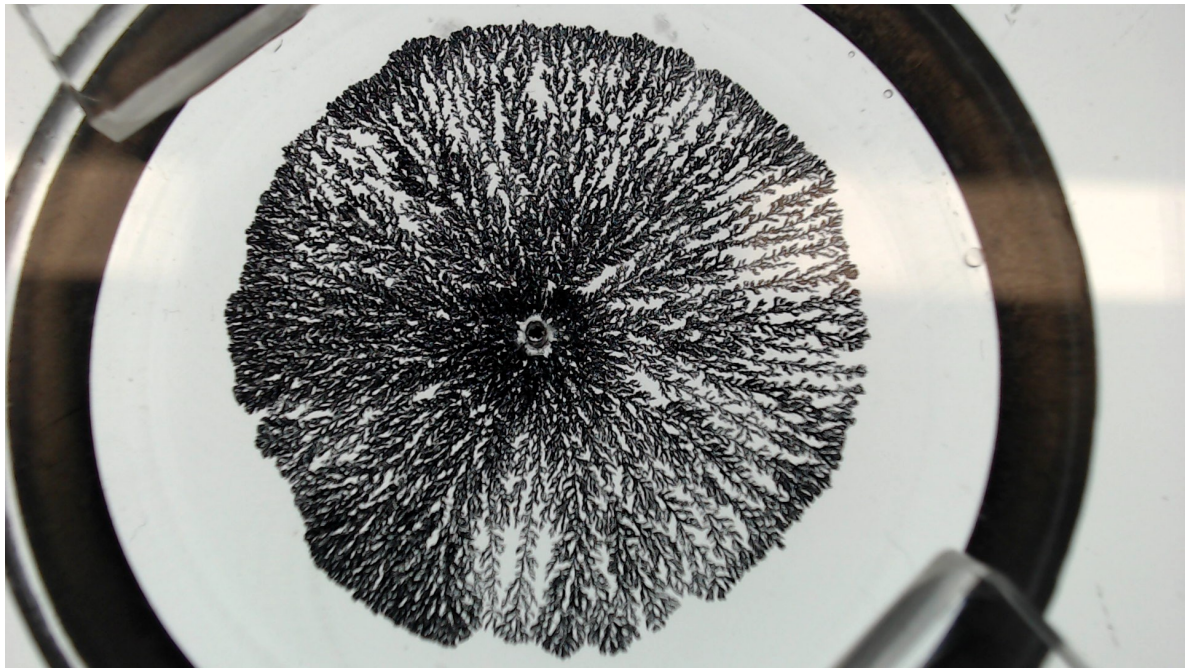
0.1M @ 20V, Centre: (391,251)  
Dendritic Structure



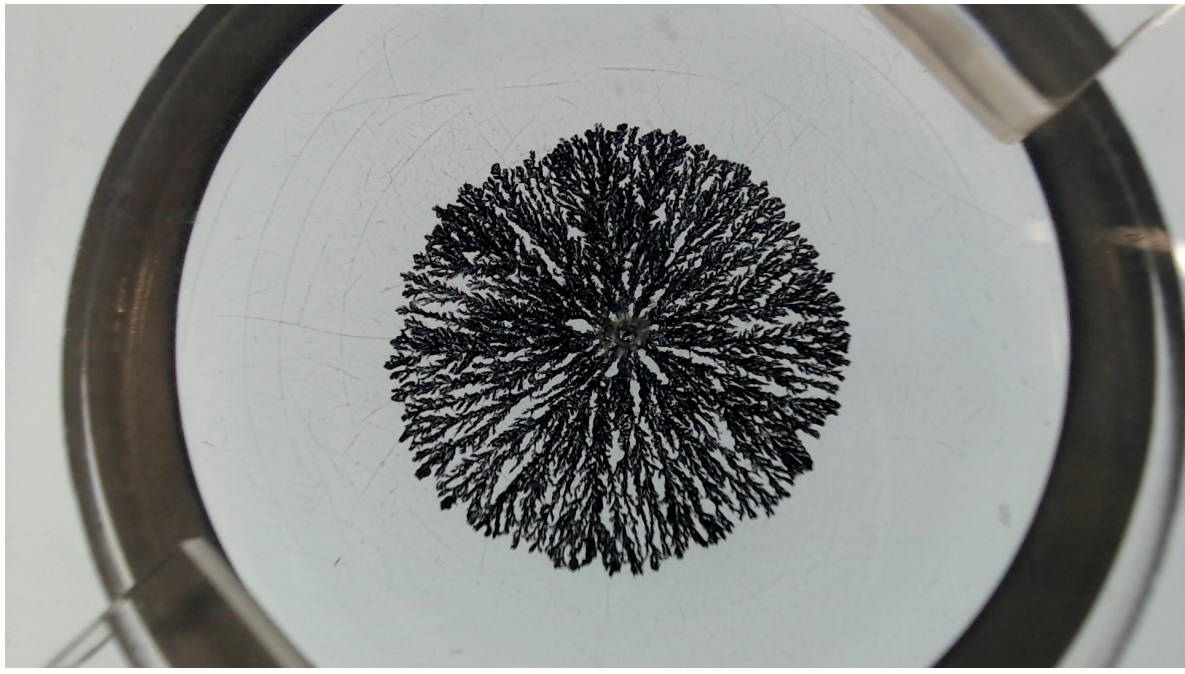
0.1M @ 30V, Centre: (496,378)  
Dendritic Structure



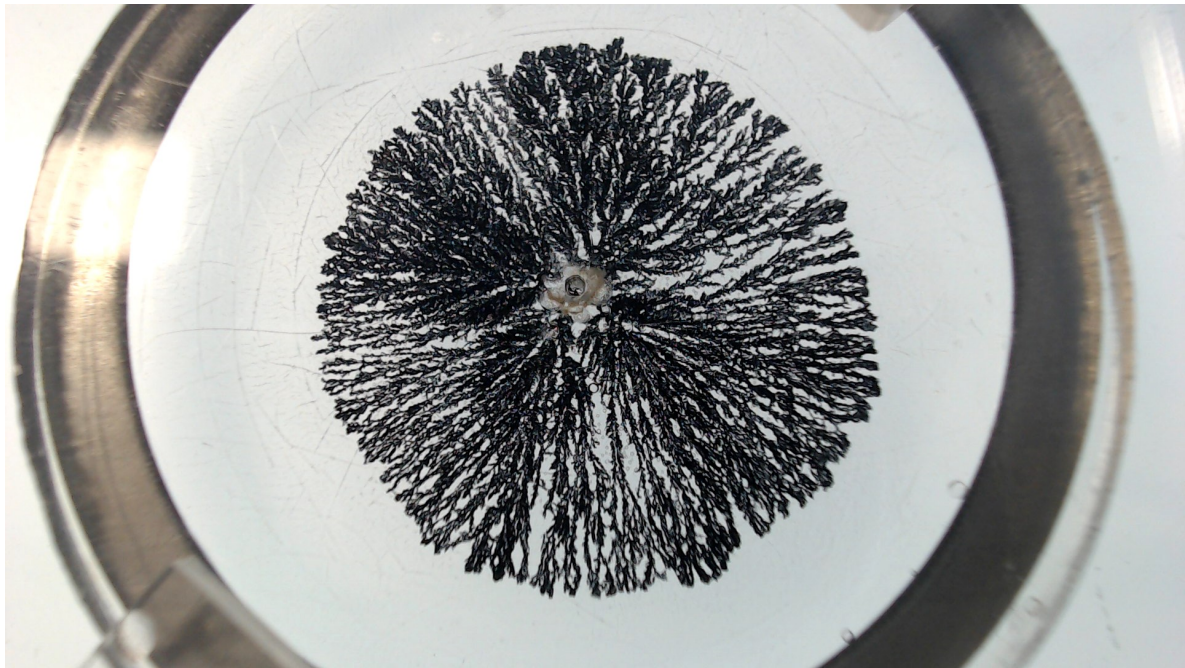
0.01M @ 5V, Centre: (5417,285)  
Diffusion-Limited Aggregation



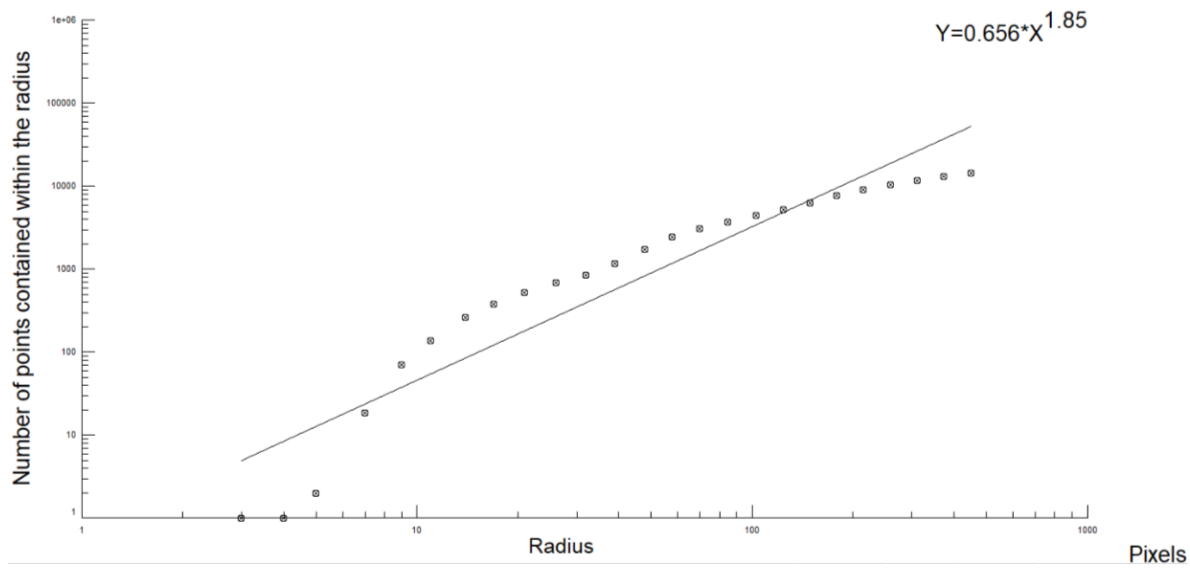
0.01M @ 10V, Centre: (668,518)  
Dense Radial Structure



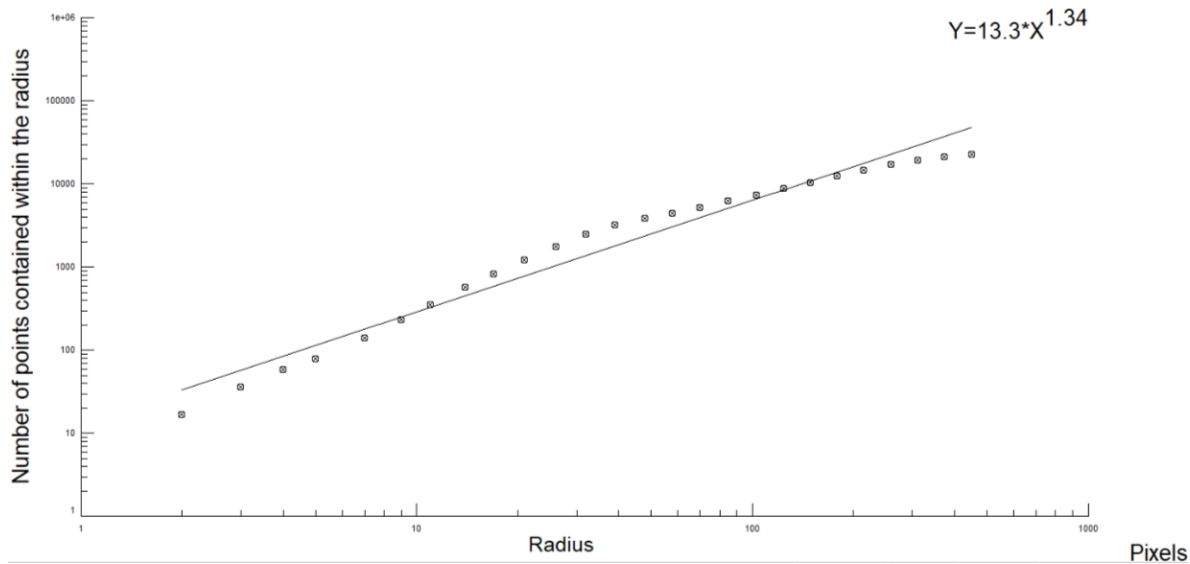
0.01M @ 20V, Centre: (513,349)  
Dense Radial Structure



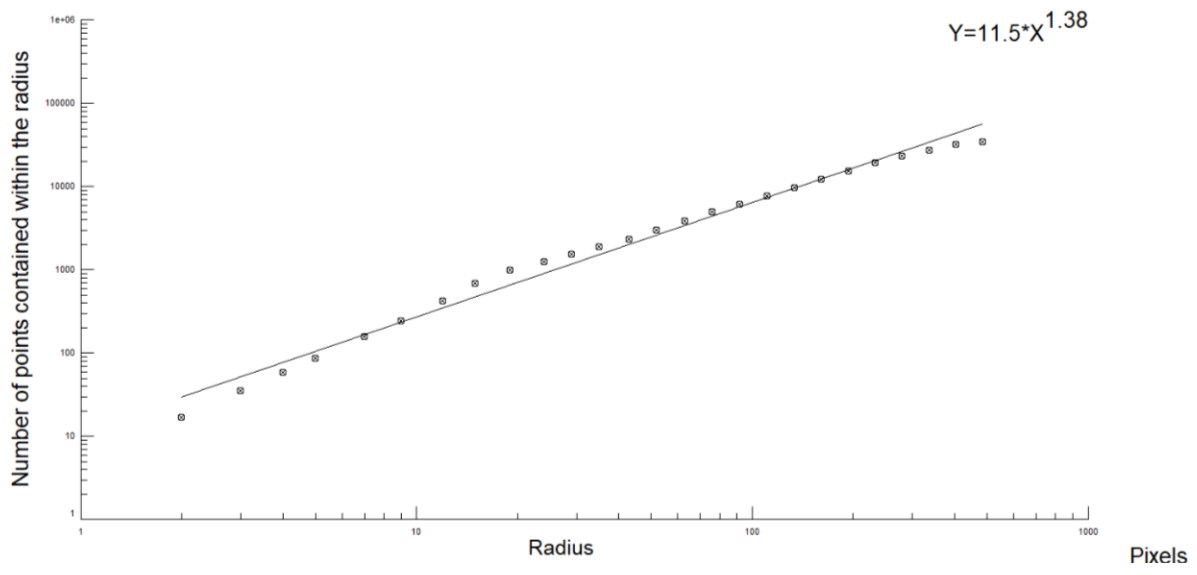
0.01M @ 30V, Centre: (572,406)  
Dense Radial Structure



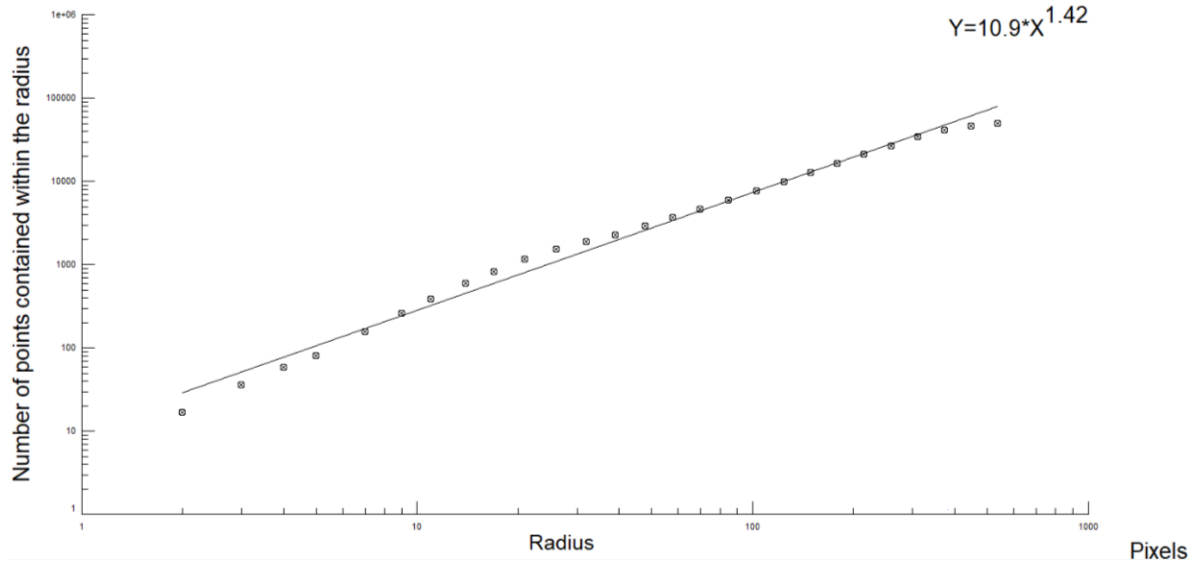
1M @ 4.5V  
Mass Comparison Fractal Dimension:  $1.8 \pm 4.4$



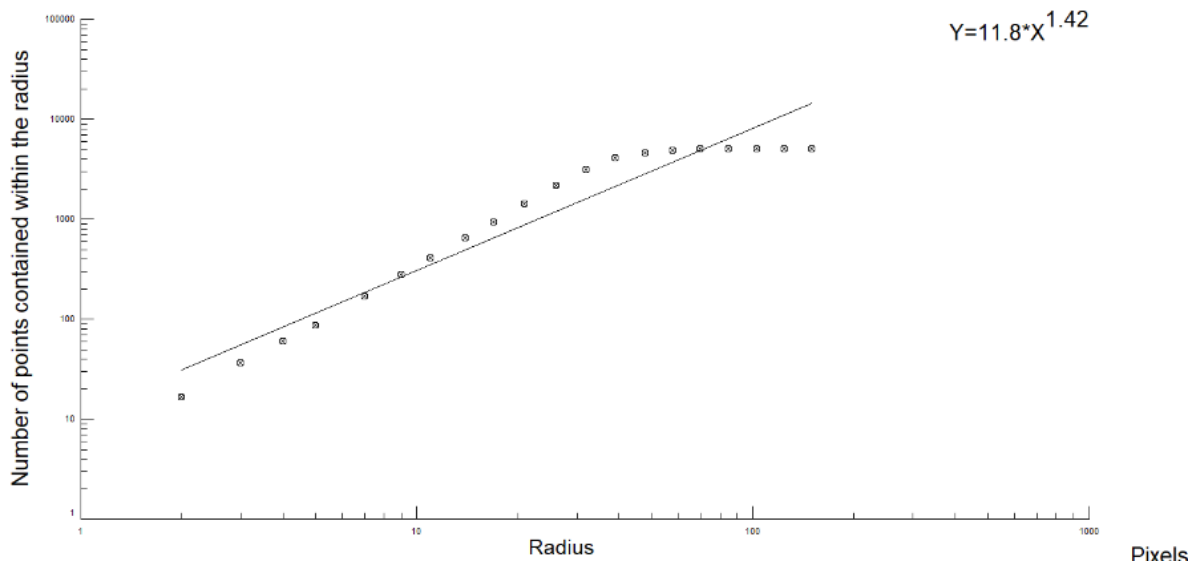
1M @ 5.0V  
Mass Comparison Fractal Dimension:  $1.3 \pm 0.8$



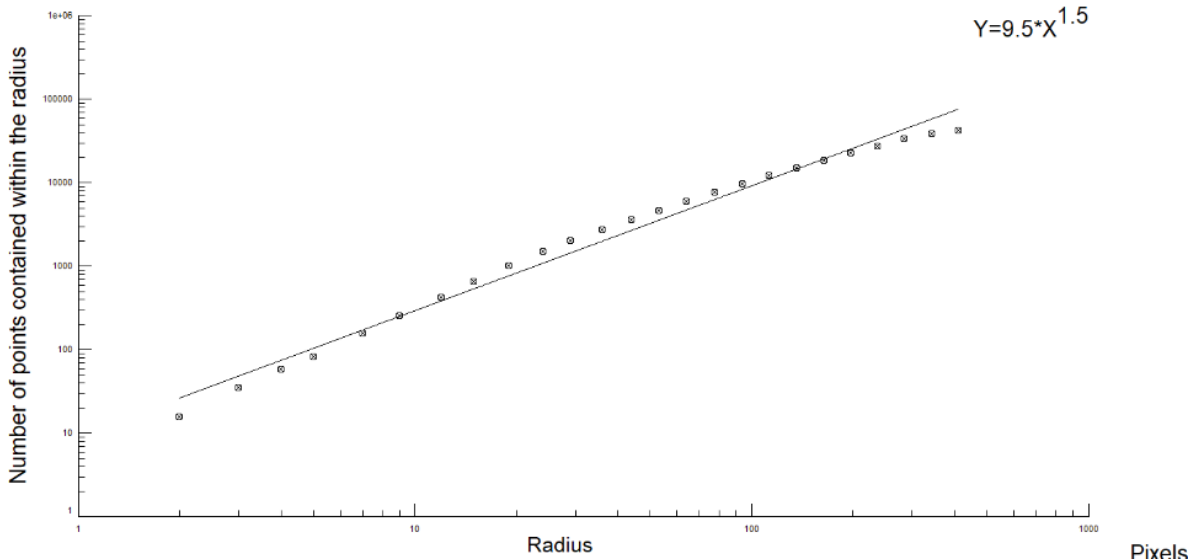
1M @ 20V  
Mass Comparison Fractal Dimension:  $1.4 \pm 0.3$



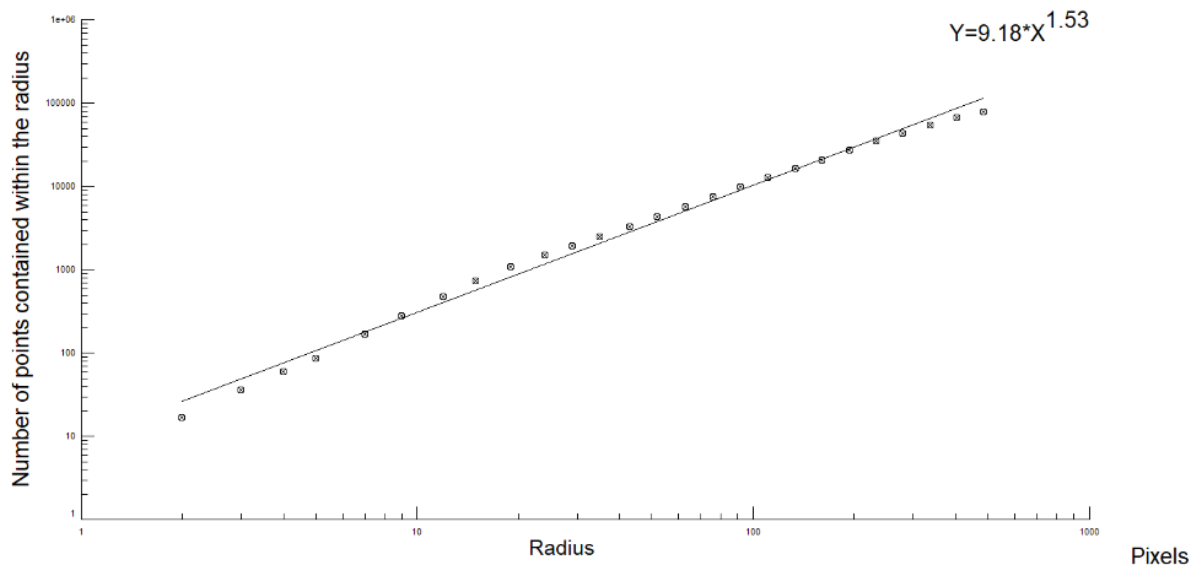
1M @ 30V  
Mass Comparison Fractal Dimension:  $1.4 \pm 0.3$



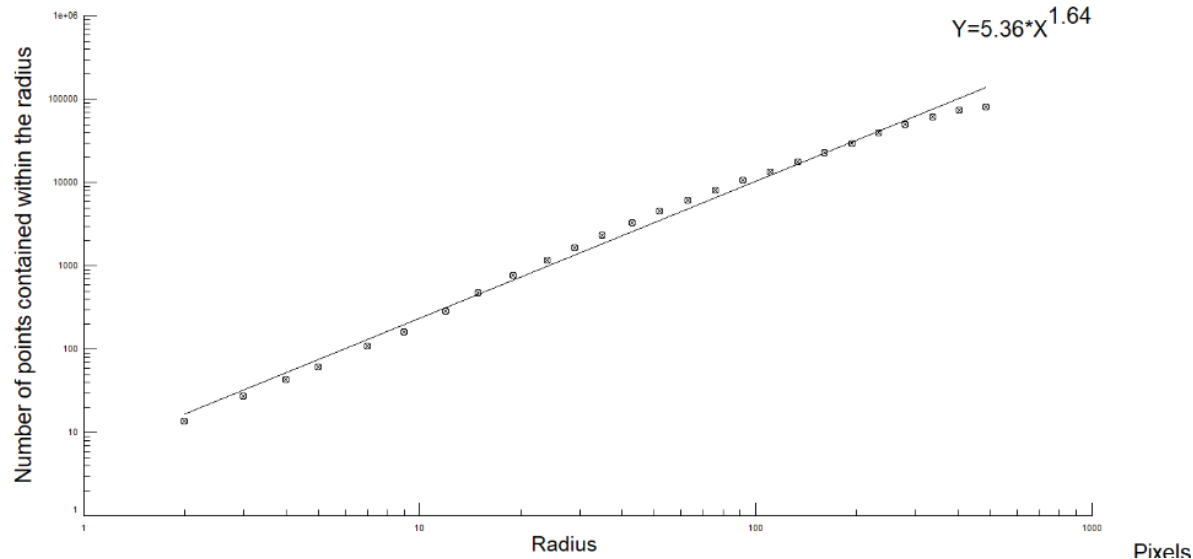
1M @ 0.0 → 2.5V  
 Mass Comparison Fractal Dimension:  $1.4 \pm 0.9$



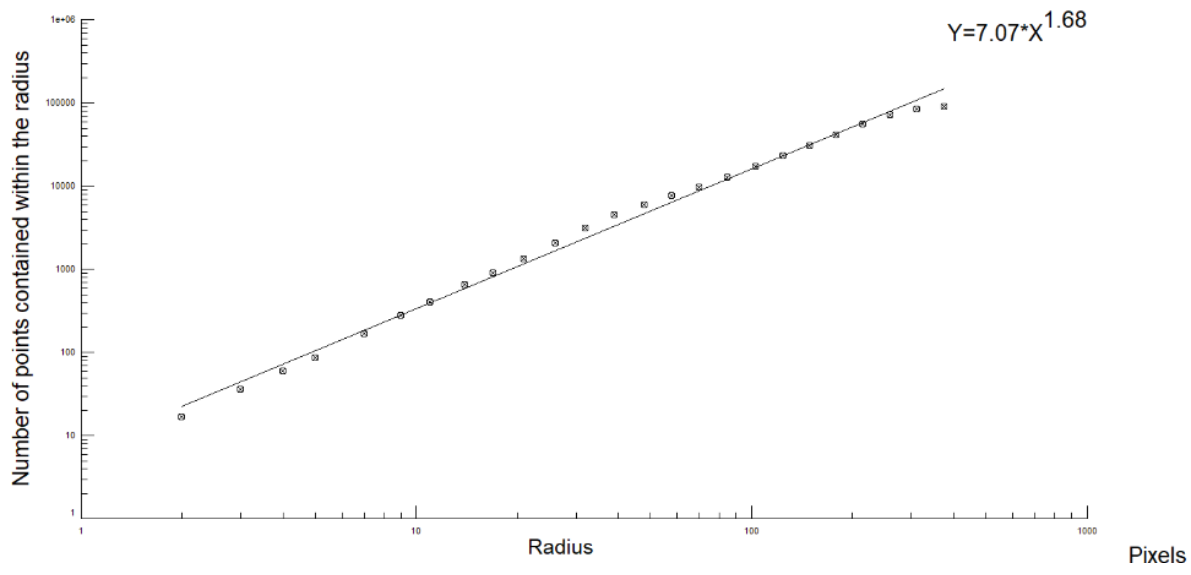
0.5M @ 10V  
 Mass Comparison Fractal Dimension:  $1.5 \pm 0.4$



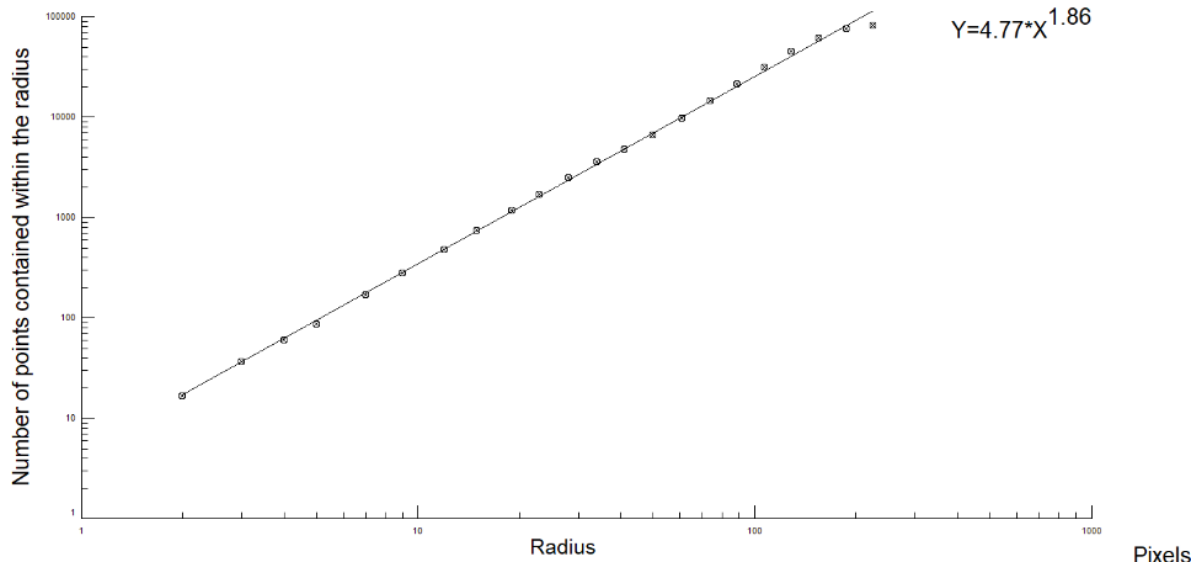
0.5M @ 20V  
 Mass Comparison Fractal Dimension:  $1.5 \pm 0.2$



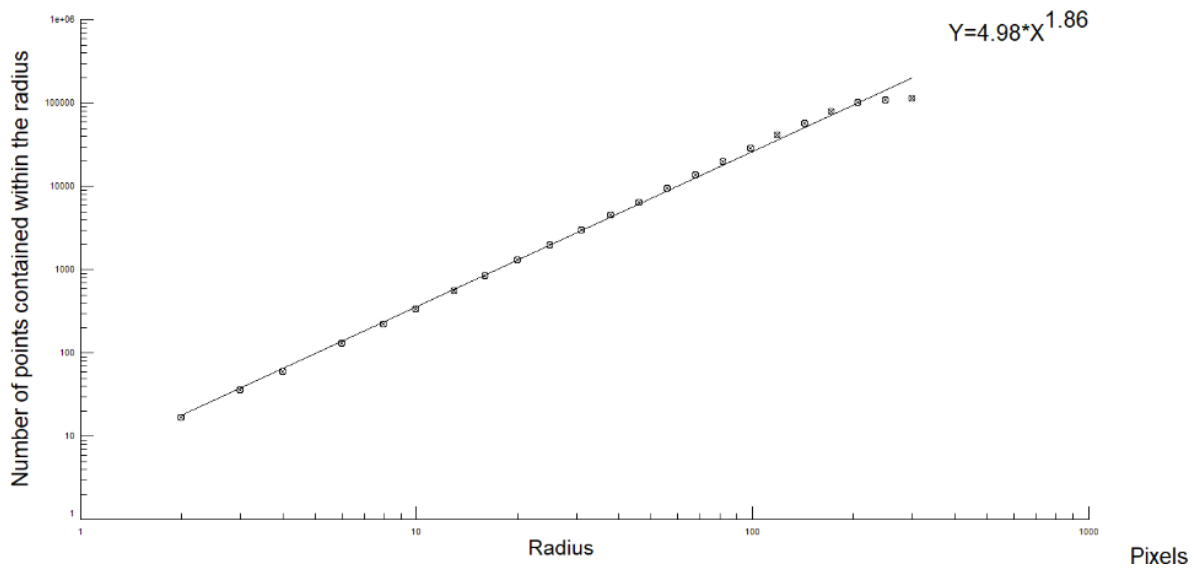
0.5M @ 30V  
 Mass Comparison Fractal Dimension:  $1.6 \pm 0.2$



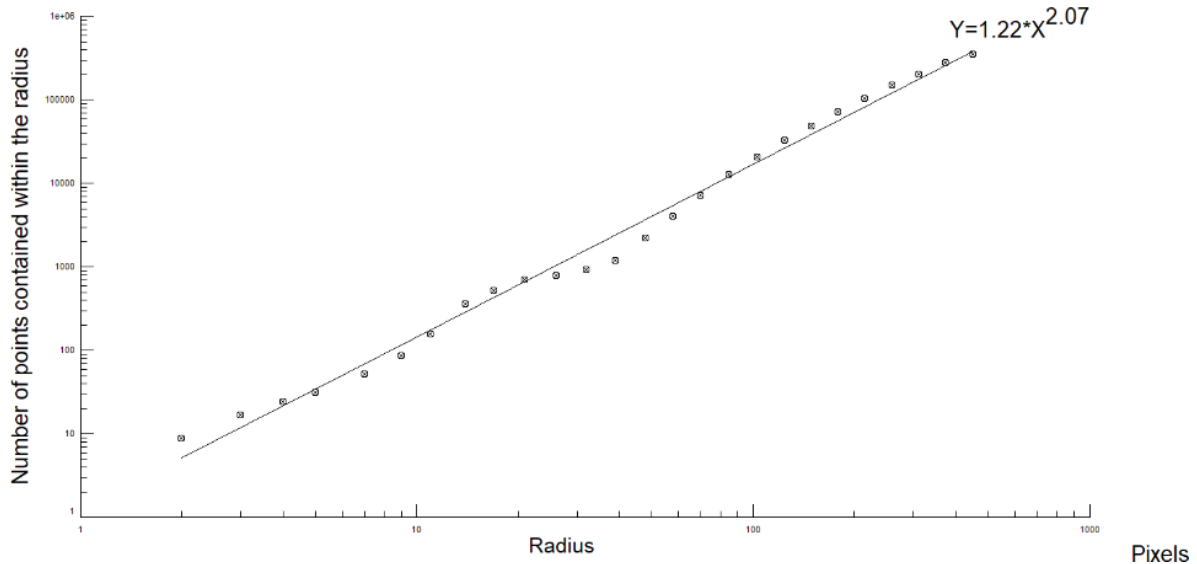
0.1M @ 5V  
 Mass Comparison Fractal Dimension:  $1.7 \pm 0.2$



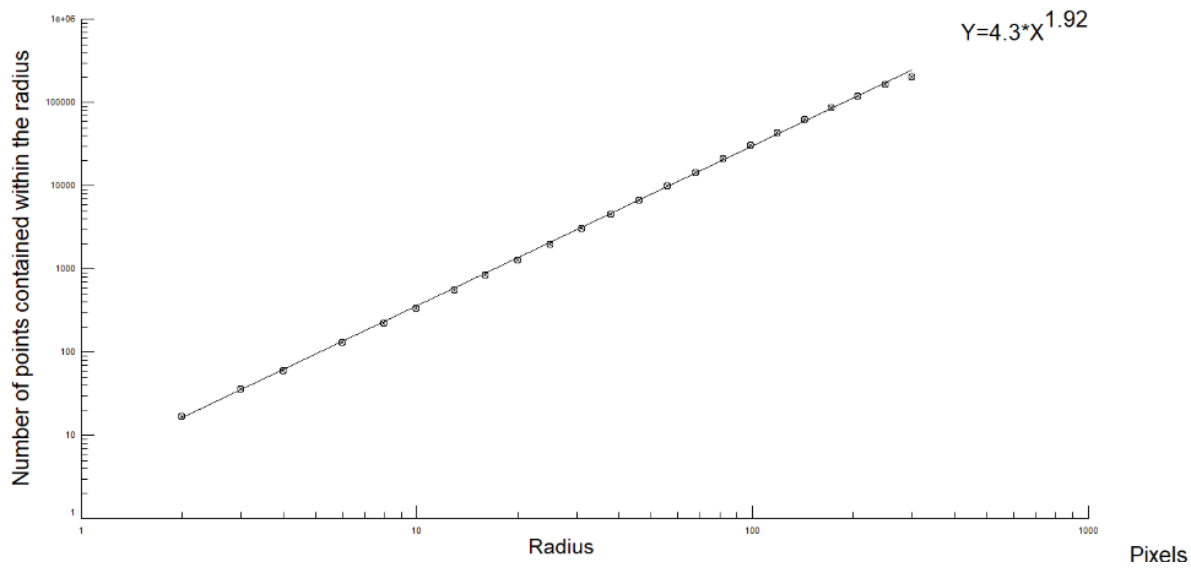
0.1M @ 10V  
 Mass Comparison Fractal Dimension:  $1.86 \pm 0.03$



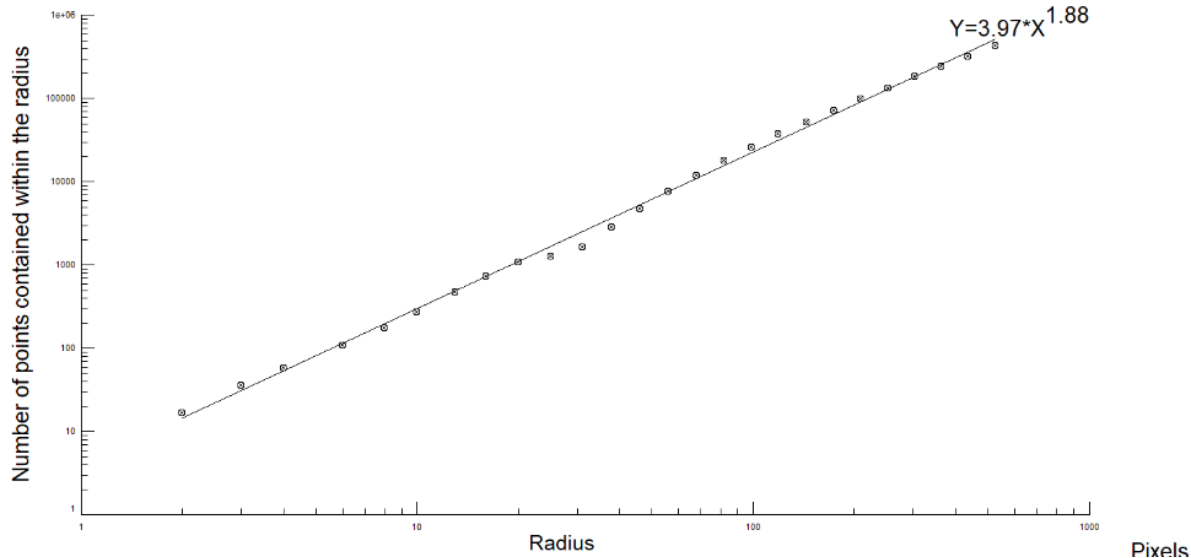
0.1M @ 20V  
Mass Comparison Fractal Dimension:  $1.86 \pm 0.09$



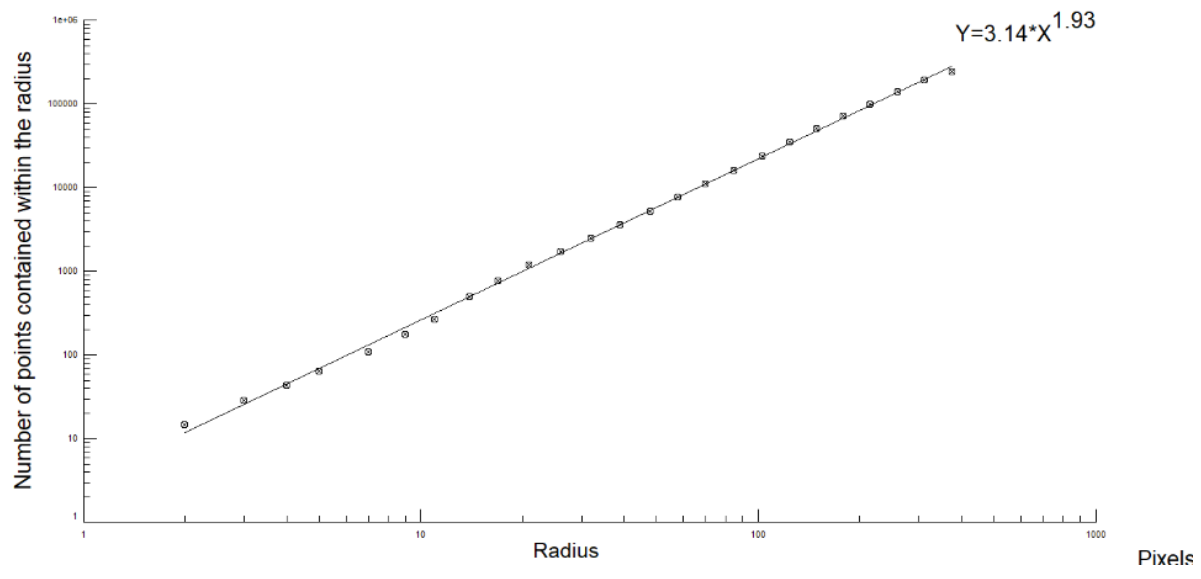
0.1M @ 30V  
Mass Comparison Fractal Dimension:  $1.9 \pm 0.01$



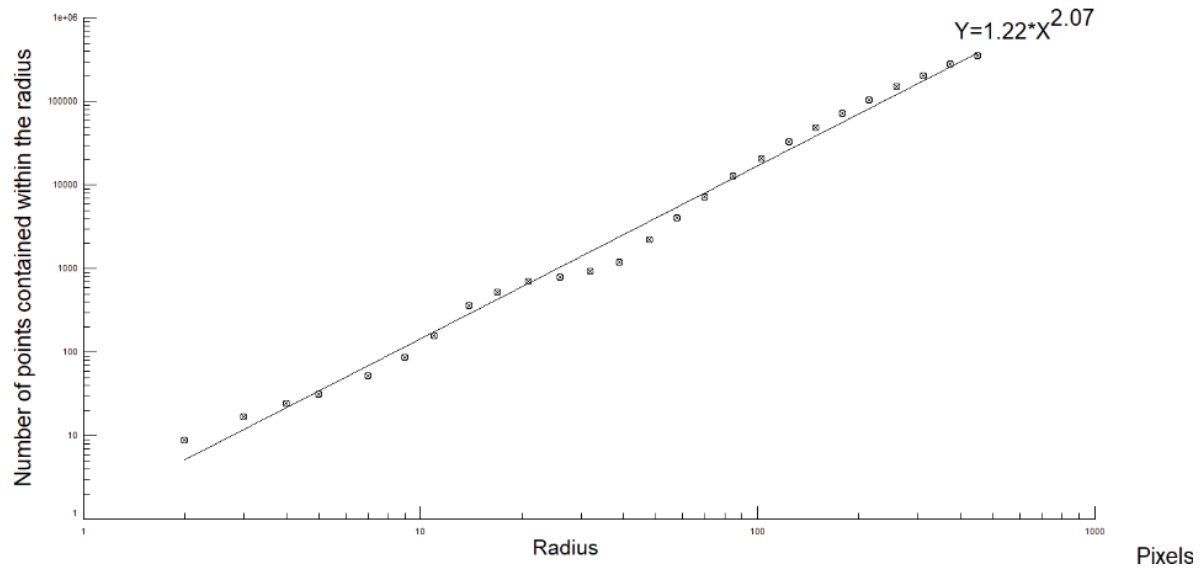
0.01M @ 5V  
Mass Comparison Fractal Dimension:  $1.92 \pm 0.02$



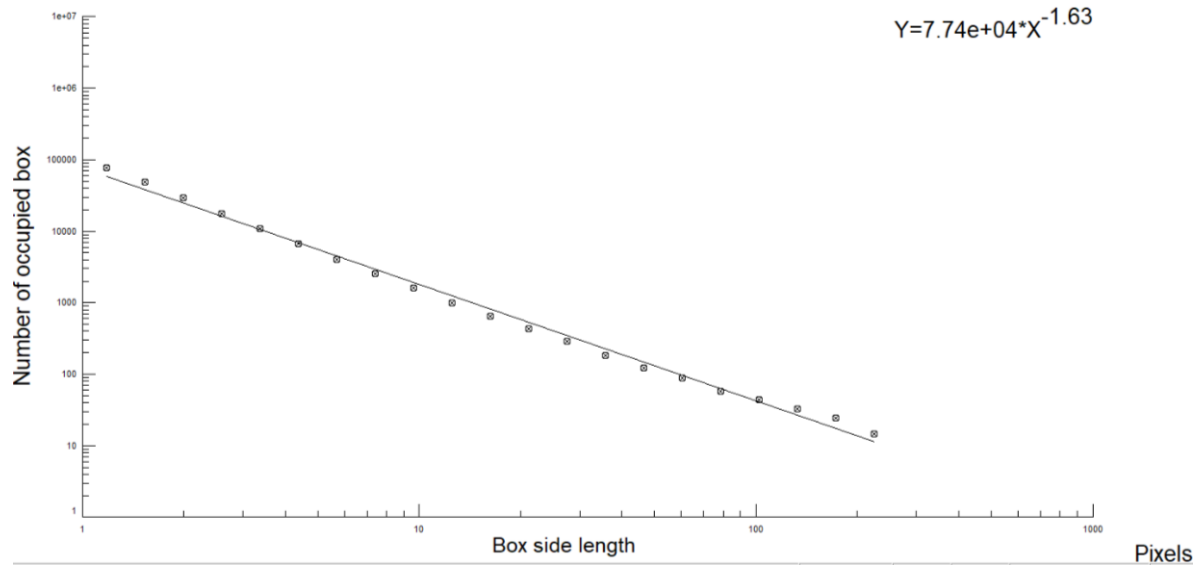
0.01M @ 10V  
Mass Comparison Fractal Dimension:  $1.9 \pm 0.1$



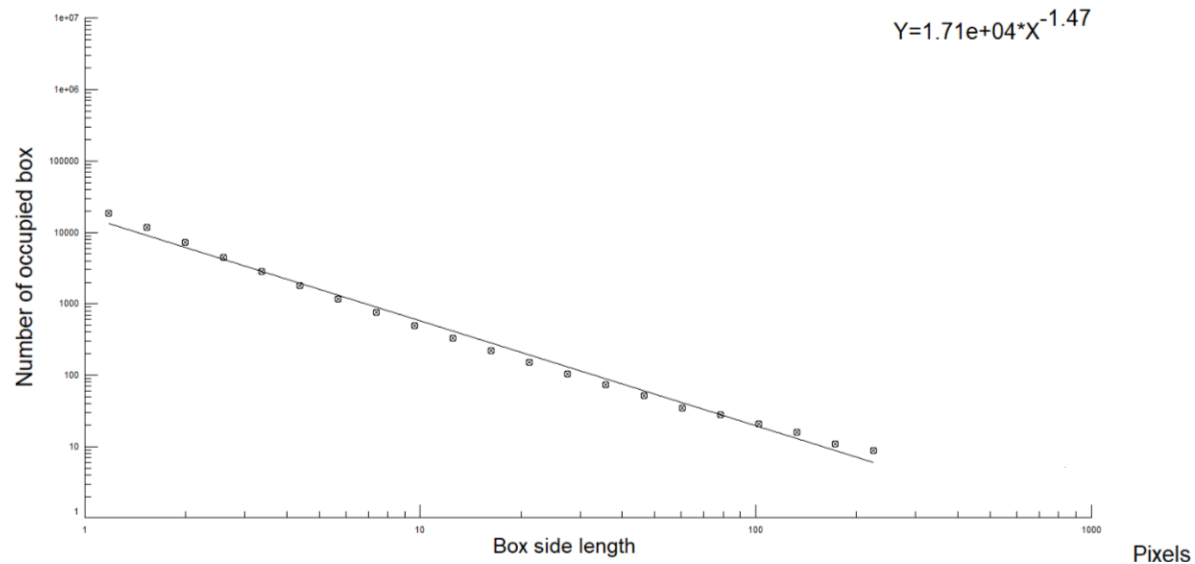
0.01M @ 20V  
Mass Comparison Fractal Dimension:  $1.93 \pm 0.04$



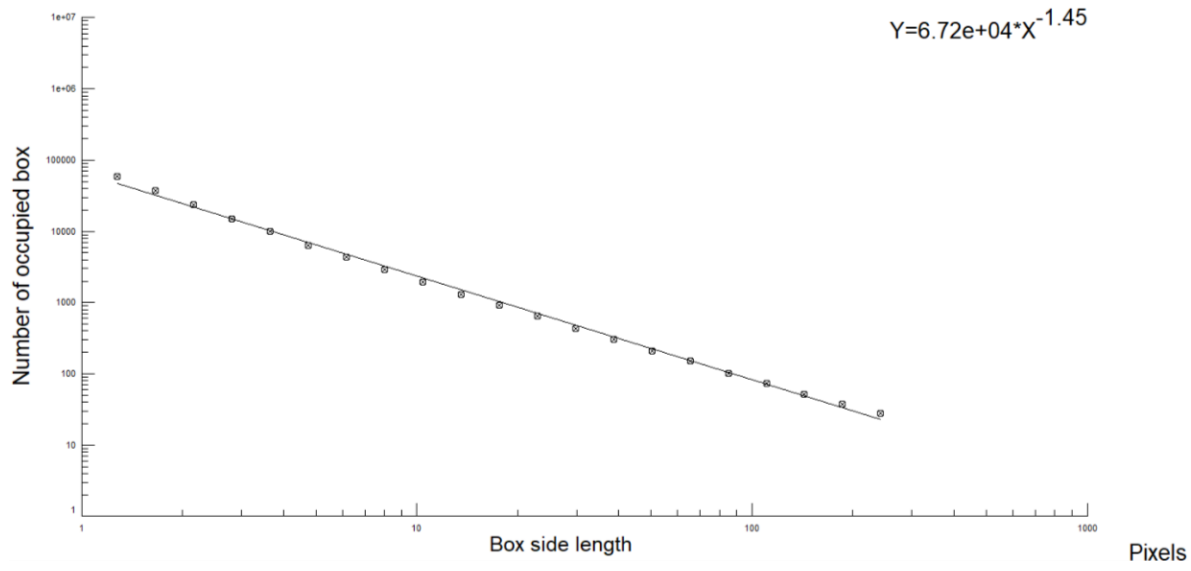
0.01M @ 30V  
Mass Comparison Fractal Dimension:  $2.1 \pm 0.4$



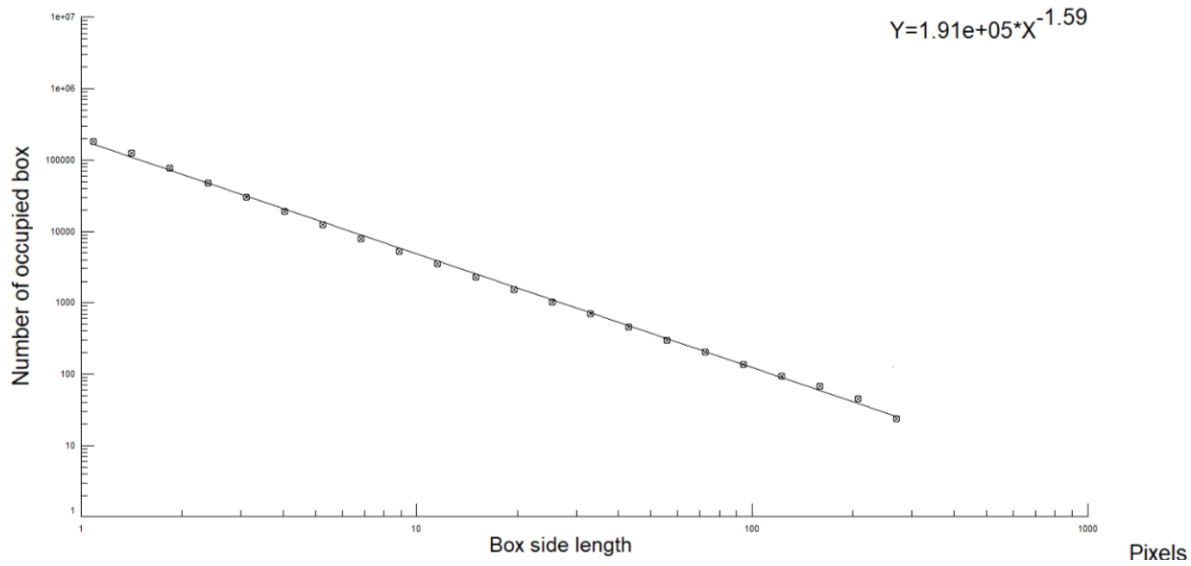
1M @ 4.5V  
Box Counting Fractal Dimension:  $1.6 \pm 0.1$



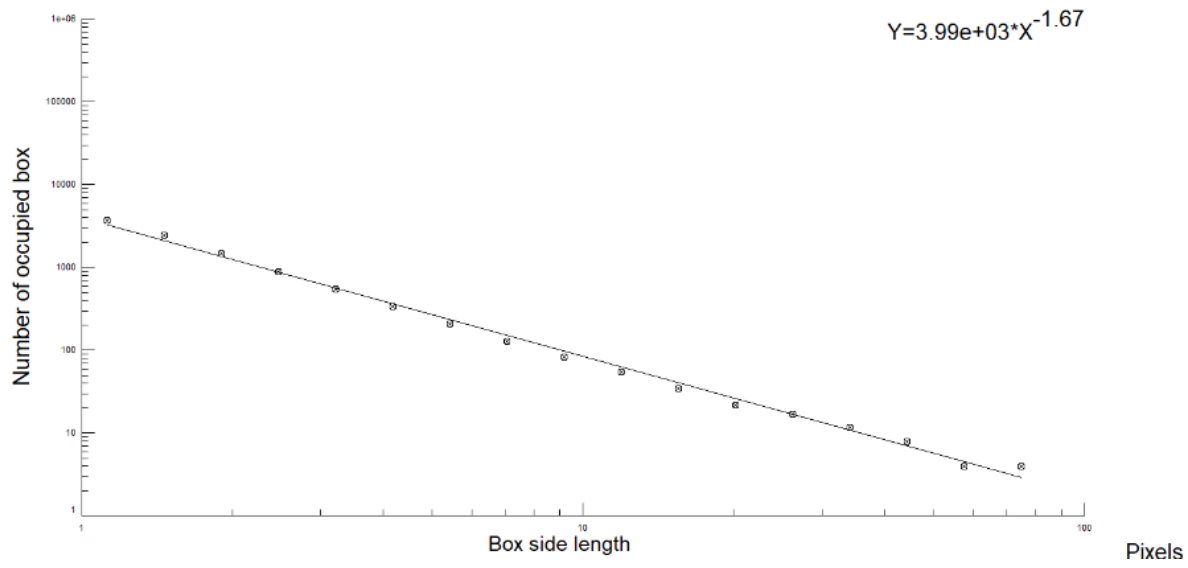
1M @ 5.0V  
Box Counting Fractal Dimension:  $1.4 \pm 0.1$



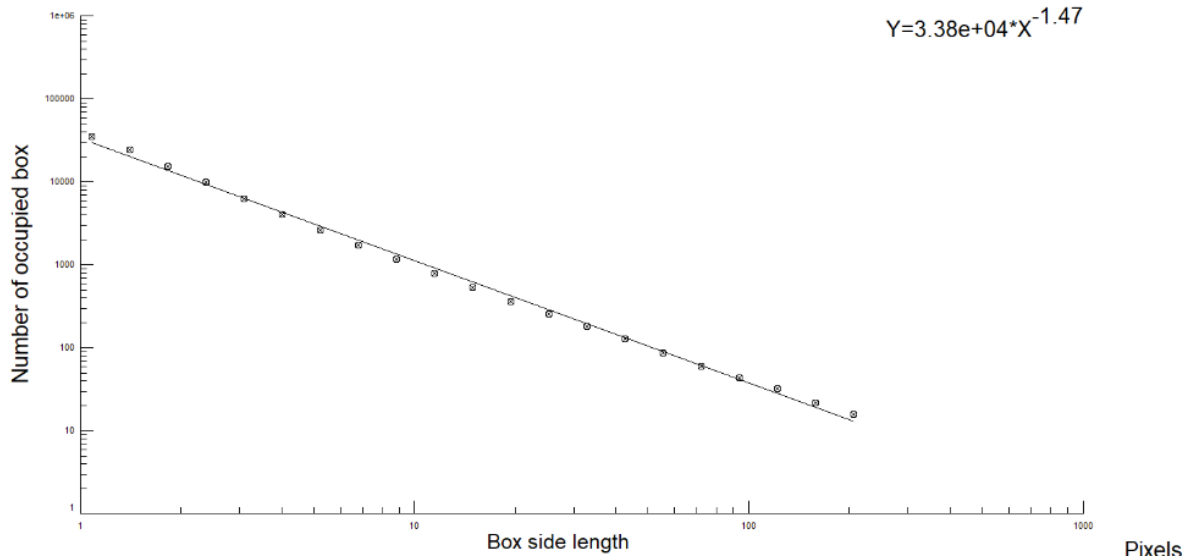
1M @ 20V  
Box Counting Fractal Dimension:  $1.45 \pm 0.05$



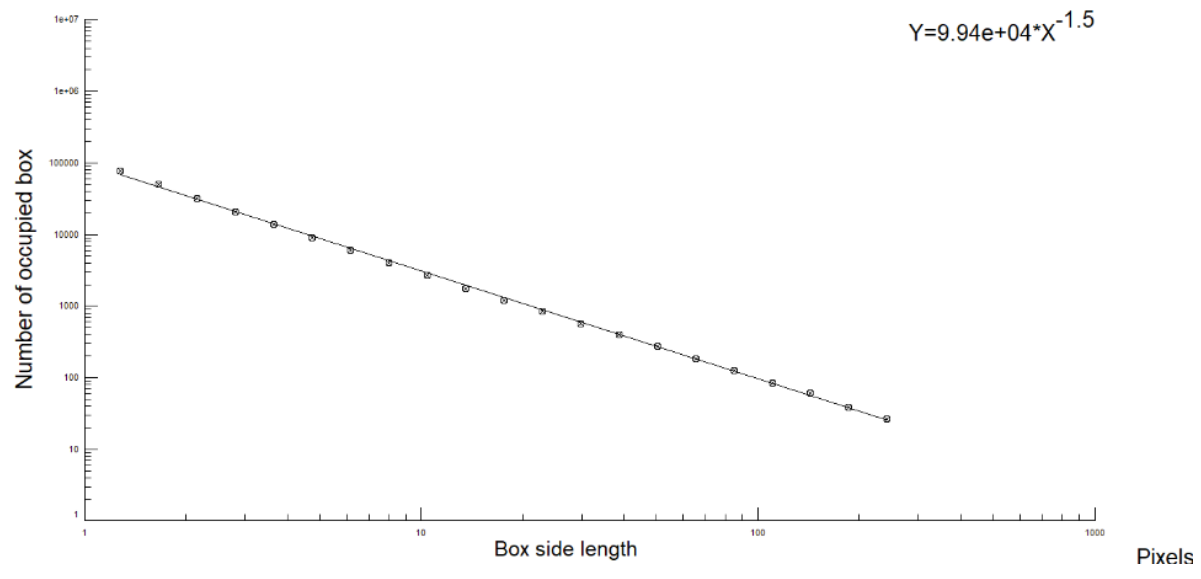
1M @ 30V  
Box Counting Fractal Dimension:  $1.59 \pm 0.03$



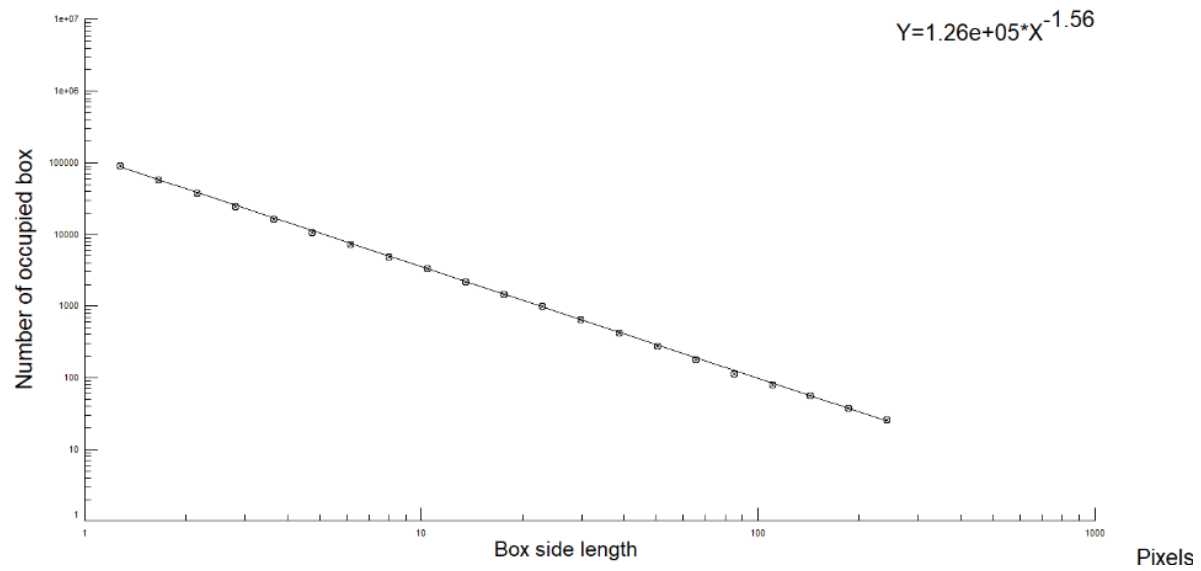
1M @ 0.0→2.5V  
Box Counting Fractal Dimension:  $1.68 \pm 0.06$



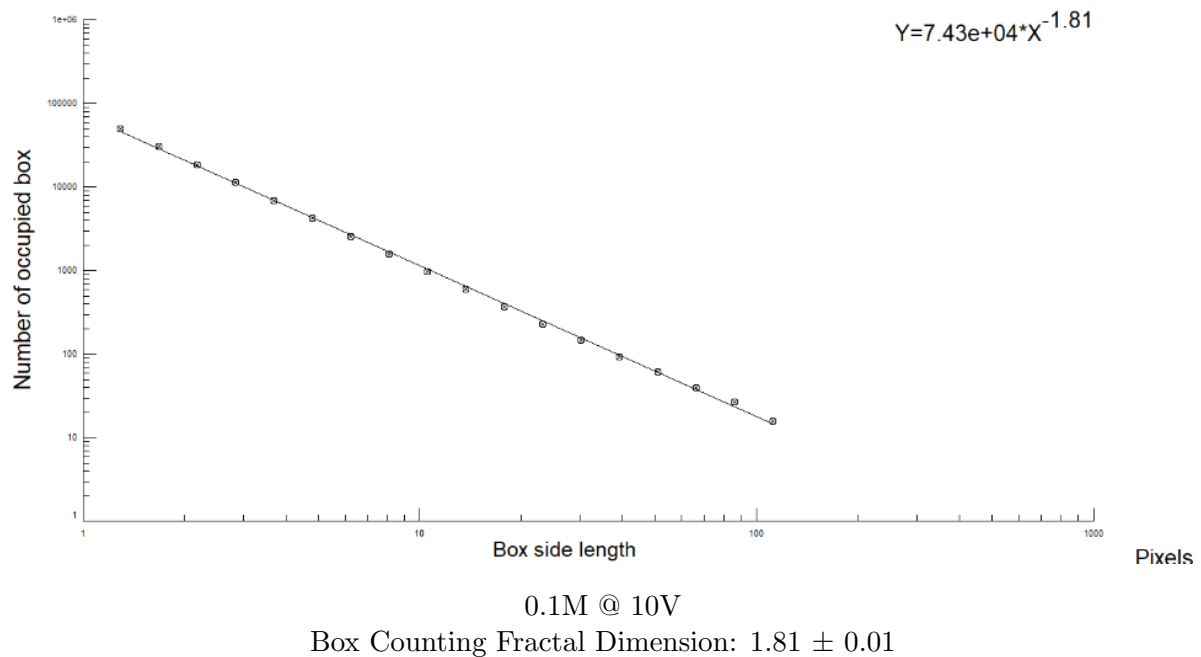
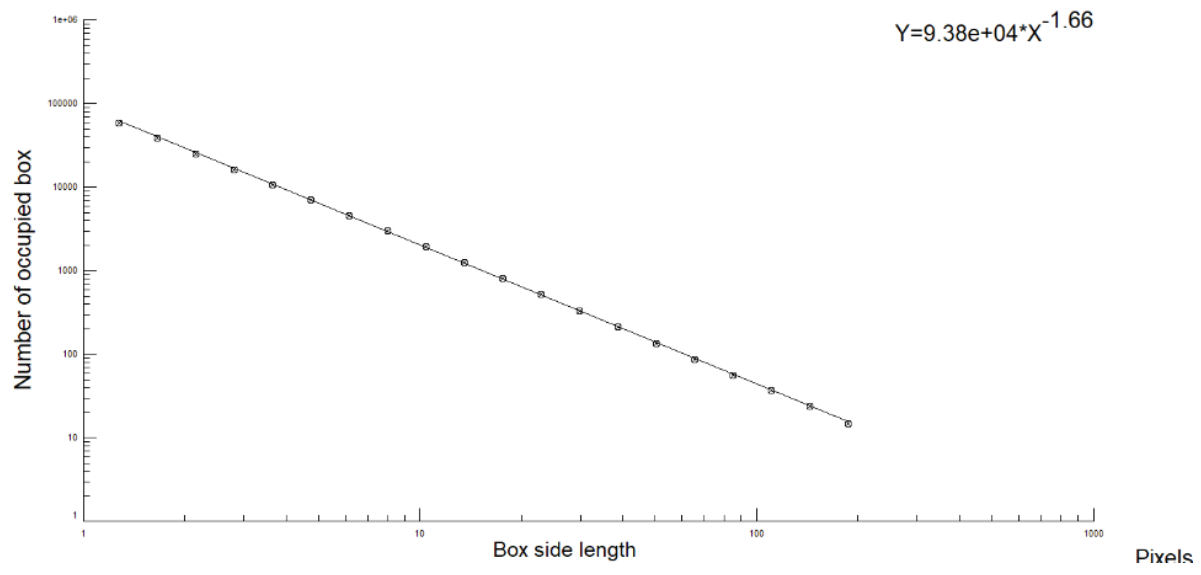
0.5M @ 10V  
Box Counting Fractal Dimension:  $1.47 \pm 0.06$

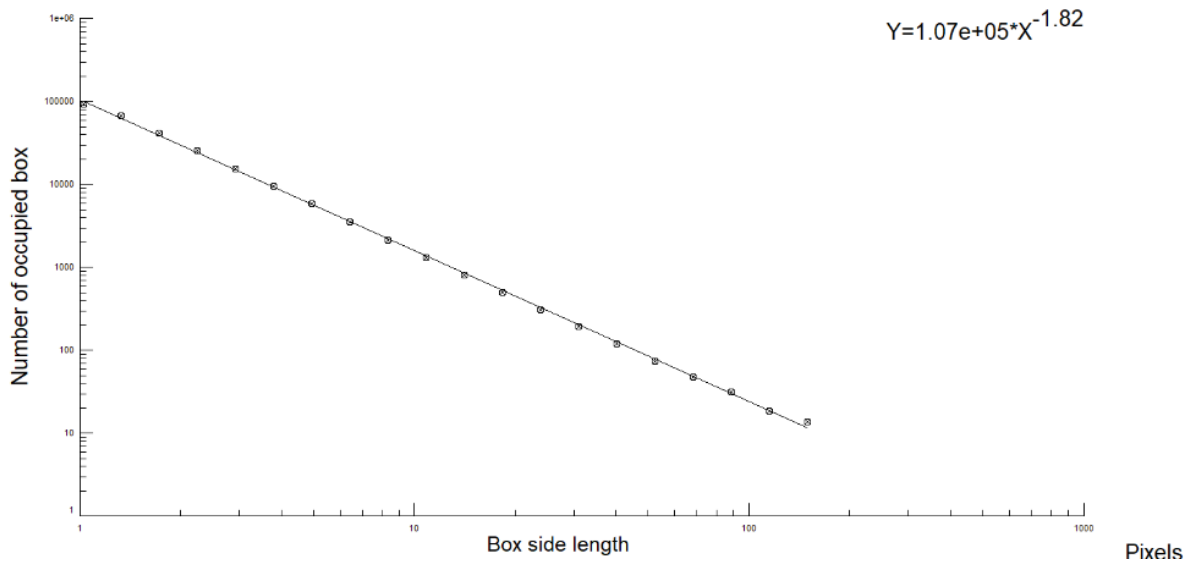


0.5M @ 20V  
Box Counting Fractal Dimension:  $1.82 \pm 0.01$

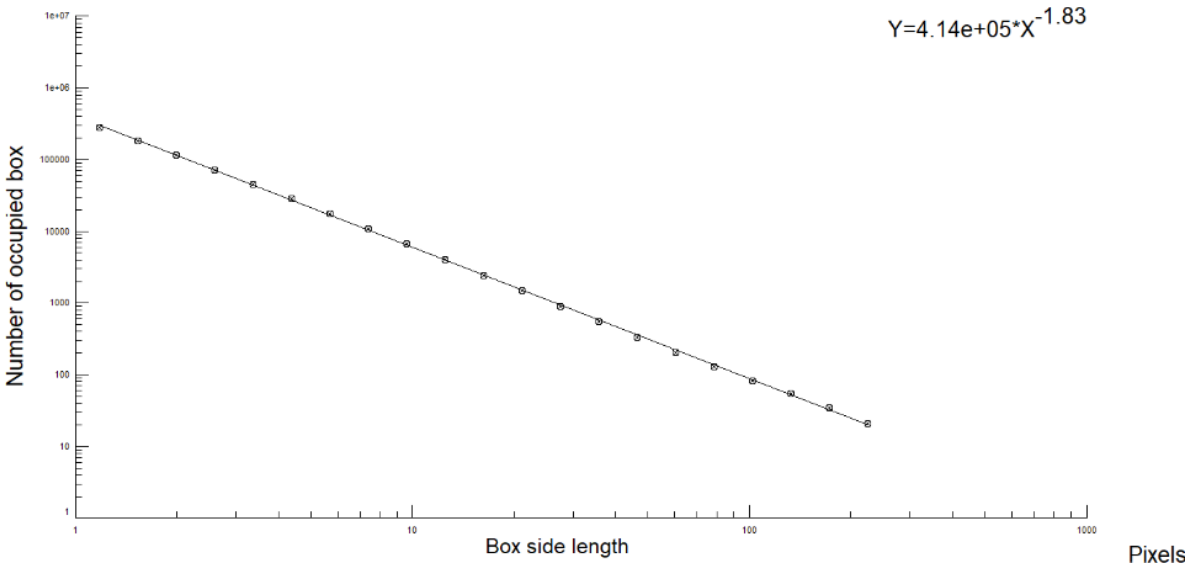


0.5M @ 30V  
Box Counting Fractal Dimension:  $1.55 \pm 0.005$

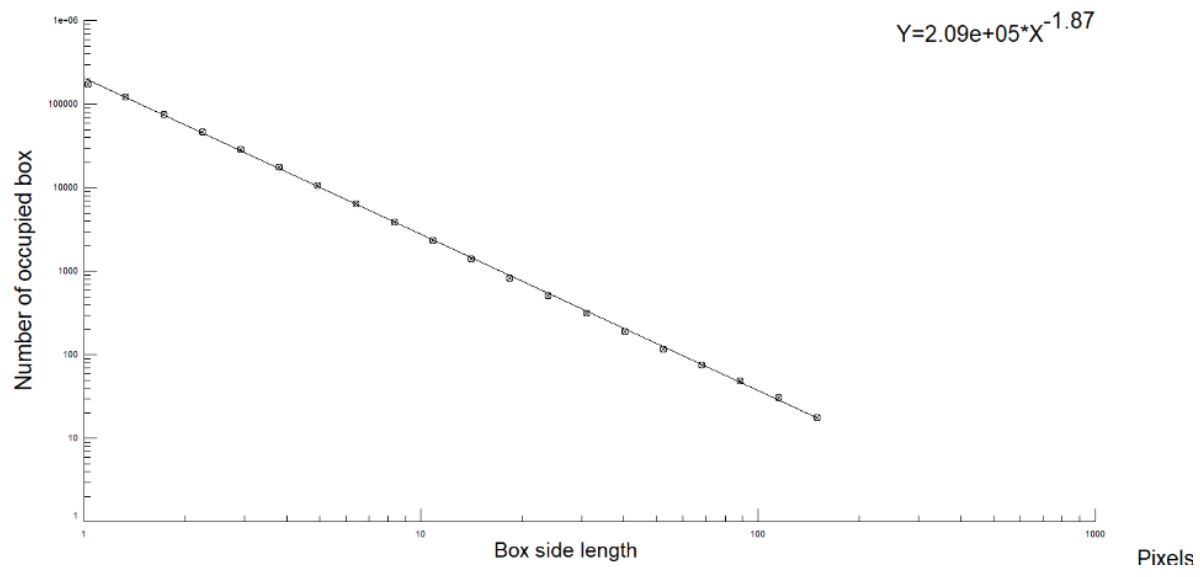




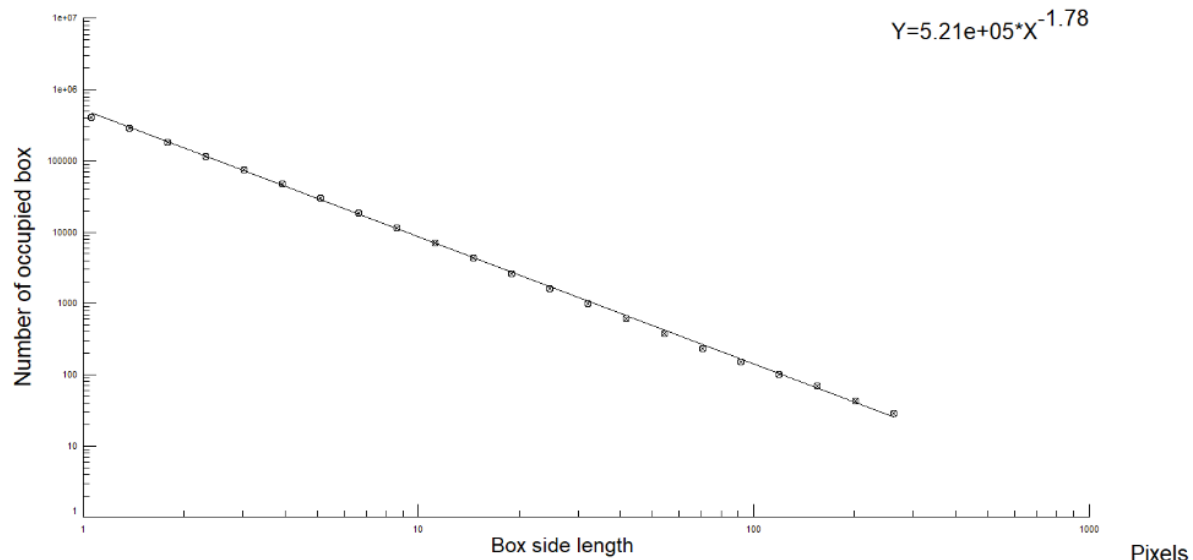
0.1M @ 20V  
Box Counting Fractal Dimension:  $1.82 \pm 0.01$



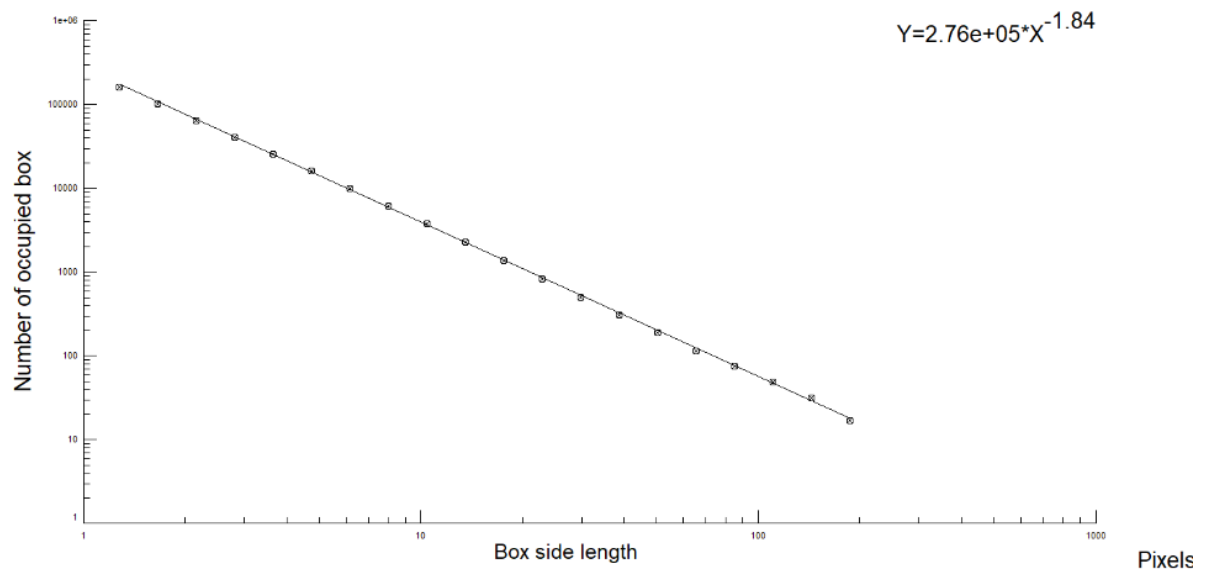
0.1M @ 30V  
Box Counting Fractal Dimension:  $1.797 \pm 0.006$



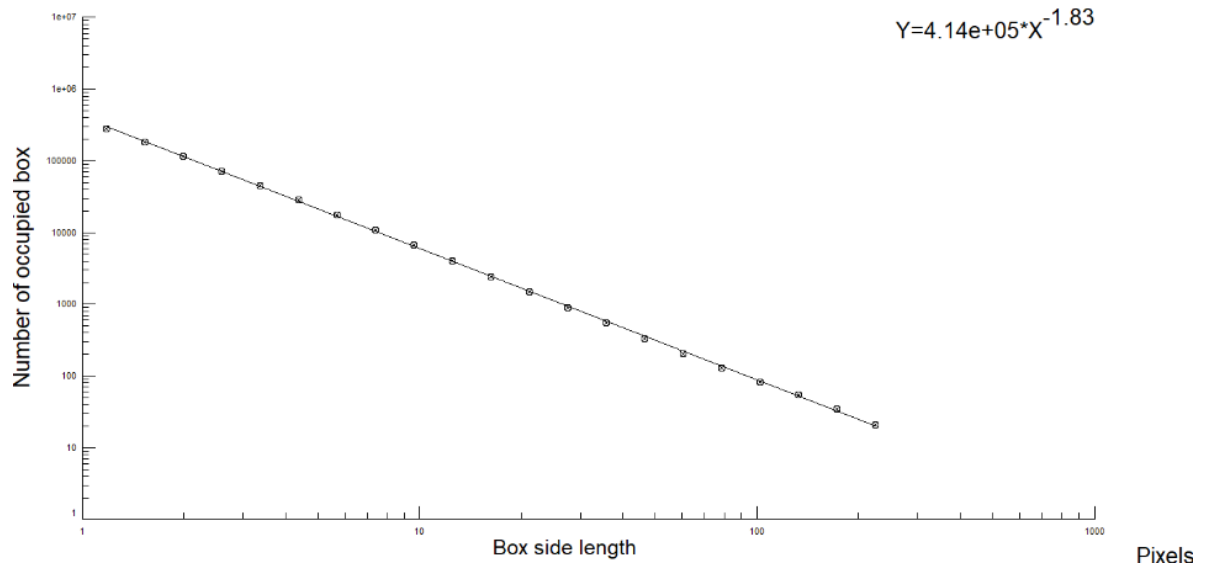
0.01M @ 5V  
Box Counting Fractal Dimension:  $1.872 \pm 0.009$



0.01M @ 10V  
Box Counting Fractal Dimension:  $1.78 \pm 0.02$



0.01M @ 20V  
Box Counting Fractal Dimension:  $1.842 \pm 0.008$



0.01M @ 30V  
Box Counting Fractal Dimension:  $1.833 \pm 0.009$